

FFI RAPPORT

**GEOACOUSTIC INVERSION
ON THE CONTINENTAL SHELF:
LAYERED ELASTIC SEABEDS**

TOLLEFSEN Dag

FFI/RAPPORT-2002/04608

FFIBM/836/116

Approved
Horten 5 December 2002

J K Johnsen
Director of Research

**GEOACOUSTIC INVERSION ON THE
CONTINENTAL SHELF:
LAYERED ELASTIC SEABEDS**

TOLLEFSEN Dag

FFI/RAPPORT-2002/04608

FORSVARETS FORSKNINGSINSTITUTT
Norwegian Defence Research Establishment
P O Box 25, NO-2027 Kjeller, Norway

FORSVARETS FORSKNING SINSTITUTT (FFI)
Norwegian Defence Research Establishment

UNCLASSIFIED

P O BOX 25
 NO-2027 KJELLER, NORWAY
REPORT DOCUMENTATION PAGE

SECURITY CLASSIFICATION OF THIS PAGE
 (when data entered)

1) PUBL/REPORT NUMBER FFI/RAPPORT-2002/04608	2) SECURITY CLASSIFICATION UNCLASSIFIED	3) NUMBER OF PAGES 56
1a) PROJECT REFERENCE FFIBM/836/116	2a) DECLASSIFICATION/DOWNGRADING SCHEDULE -	
4) TITLE GEOACOUSTIC INVERSION ON THE CONTINENTAL SHELF: LAYERED ELASTIC SEABEDS		
5) NAMES OF AUTHOR(S) IN FULL (surname first) TOLLEFSEN Dag		
6) DISTRIBUTION STATEMENT Approved for public release. Distribution unlimited. (Offentlig tilgjengelig)		
7) INDEXING TERMS IN ENGLISH: IN NORWEGIAN:		
a) <u>Acoustic propagation</u>	a) <u>Akustisk propagasjon</u>	
b) <u>Geoacoustic inversion</u>	b) <u>Geoakustisk inversjon</u>	
c) <u>Propagation Loss</u>	c) <u>Transmisjonstap</u>	
d) <u>Continental Shelf</u>	d) <u>Kontinentalsokkelen</u>	
e) _____	e) _____	
THESAURUS REFERENCE:		
8) ABSTRACT <p>The prediction of passive low-frequency sonar conditions in shallow water requires knowledge of the composition and geoacoustic parameters of the seabed. Seabed geoacoustic parameters can be estimated by inversion of acoustic data. The use of low-frequency broadband transmission loss data recorded on a single hydrophone in the water column has been studied in this context. A set of range-independent layered elastic seabed environments including some thin-layer cases have been studied by use of synthetic data. It is found that good estimates of key geoacoustic parameters or combinations of such can be obtained by use of this kind of data. Transmission loss data acquired at two Continental Shelf sites are then used for geoacoustic inversion. Improved-match seabed models with parameter estimates in reasonable agreement with data from other geophysical methods are obtained. The results presented support the development of an improved acoustic modelling and prediction capability for the Continental Shelf.</p>		
9) DATE 5 December 2002	AUTHORIZED BY This page only J K Johnsen	POSITION Director of Research

ISBN 82-464-0684-1

UNCLASSIFIED

SECURITY CLASSIFICATION OF THIS PAGE
 (when data entered)

CONTENTS

	Page	
1	INTRODUCTION	7
2	DATA AND INVERSION TOOLS	8
2.1	Acoustic data	8
2.2	Environment data	8
2.3	Geoacoustic models	8
2.4	Inversion tools	9
2.4.1	The genetic algorithm	9
2.4.2	The propagation model	10
2.4.3	The Bartlett processor	10
2.4.4	The TL processor	11
2.4.5	Model parameters	11
2.4.6	A posteriori statistics	12
3	SYNTHETIC DATA	13
3.1	Test cases	13
3.2	Experiment configurations	14
3.3	Presentation of results	15
3.4	The EL cases	15
3.4.1	Seabed models	15
3.4.2	Results	16
3.4.3	Parameter estimates	17
3.5	The CS cases	19
3.5.1	Seabed models	19
3.5.2	Results	20
3.5.3	Parameter estimates	21
3.6	Geometric parameters	23
3.7	Summary	24
4	CONTINENTAL SHELF DATA	25
4.1	Geometry	25
4.2	Sensitivity study	25
4.3	Inversion setup	29
4.4	Site S02	29
4.4.1	Baseline model	29
4.4.2	Inversion results	30
4.4.3	Alternative models	34
4.4.4	Few frequencies	35
4.5	Site S05	37
4.5.1	Baseline model	37

4.5.2	Inversion results	38
4.5.3	Alternative models	42
4.5.4	Inversion in segments	43
4.6	Summary	43
5	SUMMARY	44
	References	45
A	TWO-PAGE ABSTRACT	47
B	TEST CASES	49
B.1	EL cases	49
B.2	CS cases	51
C	SEABED MODELS	52
C.1	Site S02	52
C.2	Site S05	53
	DISTRIBUTION LIST	55

GEOACOUSTIC INVERSION ON THE CONTINENTAL SHELF: LAYERED ELASTIC SEABEDS¹

1 INTRODUCTION

The prediction of passive low-frequency sonar conditions in shallow water requires knowledge of the composition of the seabed, and of the effect of this on acoustic propagation. Long-range low-frequency propagation in shallow water has been a topic of research for several decades (1). For many environments, the seabed can to a good approximation be treated as a simple homogeneous fluid medium. In more complicated situations, as often encountered on the Continental Shelf, the seabed must be treated as a layered elastic medium. For all cases, it is desired to determine the geoacoustic parameters of the seabed by some measurement technique.

Estimates of seabed parameters can be obtained by matched-field inversion (MFI) of acoustic data. Several applications of MFI have been demonstrated in recent years (2,3). In most applications the acoustic pressure field as measured by an array, typically a vertical array in the water column, is used. The use of transmission loss data has also attracted some interest. Heard et al (4) inverted narrow- and broadband transmission loss data to obtain seabed parameters for a number of synthetic test cases. Abrahamsson and Anderson (5) developed tools to invert data in a range-dependent environment and applied this to narrowband transmission loss data in shallow water. Pihl et al (6) developed a method for on-site determination of geoacoustic parameters by inversion of TL data on a vertical array and applied this to a data set from the Baltic. Except for Ref. 5, these studies used a range-independent fluid description of the seabed.

The present report studies use of transmission loss data for geoacoustic inversion with application to Continental Shelf seabed environments. Typical environments, both of soft elastic seabed type and anomalous environments with combinations of thin sediment and hard bedrock layers are treated.

Aspects of the acoustic data, geoacoustic models and an inversion method are outlined in Chapter 2. Synthetic data is used for inversion in Chapter 3, with both the transmission loss processor and Bartlett processor applied. Transmission loss data from two Continental Shelf sites is used for inversion in Chapter 4. Results are summarised in Chapter 5. A two-page abstract and additional results are found in the Appendix.

¹ Work presented at the First International Conference "Inverse Problems: Modeling and Simulation", Fethiye, Turkey, July 14-21 2002.

2 DATA AND INVERSION TOOLS

Matched-field inversion traditionally employs the use of narrow- or broadband acoustic pressure field data measured at an acoustic array of some vertical or horizontal aperture. The measured field is correlated with synthetic data generated by an acoustic propagation code for a model environment. Candidate seabed models are searched over in an optimisation process until a correlation or “match” of sufficient quality has been obtained. The (complex) spatial structure of the acoustic field along the array is then exploited. Transmission loss (TL) data can also be used for this purpose. All phase information is then discarded, and equally precise results should not be expected. This data may on the other hand require less precision in knowledge of the location of sources and array element positions. Thus, transmission loss data may provide estimates, albeit crude, of the same seabed parameters one seeks to extract using full-field data. As observed by Heard (4), the mere fact that data of this sort is widely available from decades of collection efforts warrants further attention to its use for inversion.

2.1 Acoustic data

Acoustic data has typically been collected using SUS explosives sources with data recorded at one or a few hydrophones in the water column and processed for transmission loss in 1/3-octave frequency bands from 16 Hz to 1.6 kHz. Experiments have been conducted at several locations on the Continental Shelf spanning a wide variety of seabed conditions. Data at low frequencies (16-160 Hz) from two different sites has been selected for this report. Both data sets were acquired at about 350 m water depth. Data from a single hydrophone in the water column with sources at ranges from 2 km to 20 km is considered. The total number of data points is about two hundred for each set.

2.2 Environment data

A certain amount of geophysical data has been acquired together with the acoustic data. The supporting measurements in general consist of: a measured bathymetry profile along the acoustic track, a measurement of sound speed in water at the receiver site, a seismic profile along the acoustic track and a sonobuoy refraction velocity measurement. Some of the sites visited have been subject to geophysical surveying by other institutions.

2.3 Geoacoustic models

All work in this report is done within the framework of range independent seabed geoacoustic models. A geoacoustic model as used in this report consists of:

- a water column of fixed depth and sound speed profile constant in range,
- one or two sediment layers, each with six geoacoustic parameters per layer: density, compressional (p-) and shear (s-) wave velocities, p- and s-wave attenuations and a layer thickness
- an elastic halfspace described by the same set of parameters except for thickness.

For simplicity, all geoacoustic layers are assumed to be homogeneous.

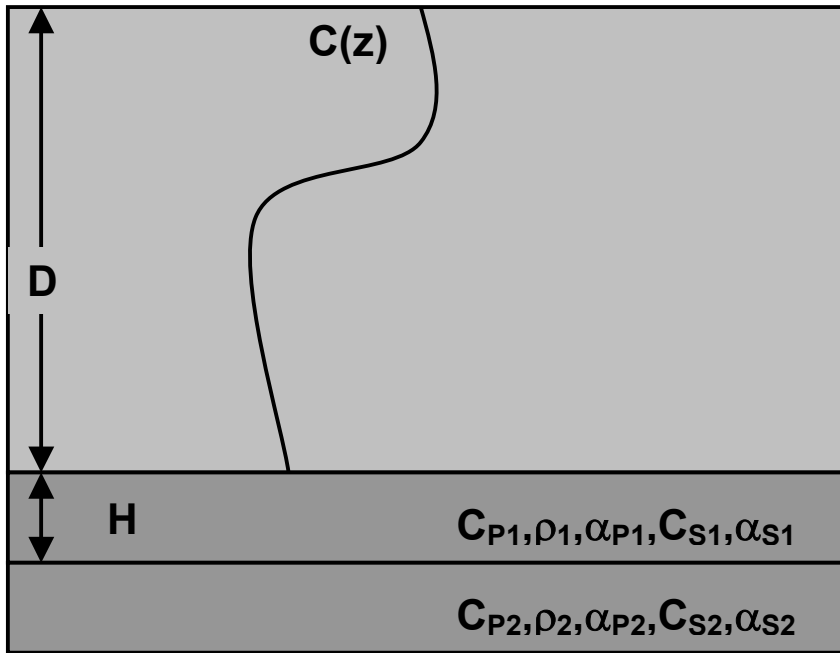


Figure 2.1 Simplified environment model consisting of a water layer (sound speed profile $c(z)$, water depth D) over a two-layer seabed (seabed parameters indicated).

A typical range-independent two-layer seabed environment model is depicted in Figure 2.1.

For surveyed areas, background or *baseline* seabed geoacoustic models have been developed from analysis of survey geophysical data and additional geophysical information. These models were used as reference when setting up the layering and geoacoustic parameter bounds for subsequent inversions. The importance of such background models for input to subsequent inversion must be stressed.

2.4 Inversion tools

Measured acoustic data is matched with synthetic (simulated) data output from some numeric acoustic propagation model for a candidate seabed geoacoustic model. The parameters of the seabed model are iterated over until an acceptable correlation or “match” is obtained - or one runs out of computer time. The iteration or search process is performed using a non exhaustive method such as simulated annealing (SA) or genetic algorithms (GA). For the present work, the genetic algorithm global search method of SAGA (7) has been used.

2.4.1 The genetic algorithm

Briefly outlined, a genetic algorithm mimics the biological evolution of a population of q members towards increased fitness. For each step in the evolution, a fraction f_q (with $0 < f < 1$) members of the population is selected and combined in pairs to generate a set of new (offspring) members. Standard crossover and mutation operators are applied. A standard choice of parameter settings has been used: crossover rate 0.80, mutation rate 0.05 and an update rate of 0.50. These settings were kept fixed during the entire inversion runs. Selection is based on a Boltzmann criterion

$$p_k = \frac{\exp[-E(m_k)/T]}{\sum_l \exp[-E(m_l)/T]} \quad (2.1)$$

where $E(m)$ is an energy function for model m_k , and T is a "temperature", gradually reduced for each step. A series of independent populations, each starting with a different set of initial members, are run in parallel. To this end, a multi-processor computer environment can be exploited.

2.4.2 The propagation model

The OASES propagation model (8) was chosen for its accuracy and its ability to handle elastic layers. The model solves for the complex wave fields in a stack of laterally homogenous fluid-solid layers bounded by vacuum above and an infinite halfspace below. The depth-separated wave equation is solved by a wavenumber integration technique, using equidistant sampling of horizontal wavenumbers over a specified interval. The far-field approximation to the Hankel function in range is used. The forward model must be called once for each frequency and source-receiver depth, then the acoustic field at all ranges is read off. Numerical parameters of the OASES model were set to:

$$c_{\min} = 1000 \text{ m/s} \quad (2.2)$$

and

$$c_{\max} = 10^8 \text{ m/s} \quad (2.3)$$

for the minimum and maximum phase velocities, and

$$NW = 4096 \quad (2.4)$$

for the wavenumber FFT length. This FFT length ensured adequate sampling to the maximum range for the highest frequency considered².

For modelling of broadband transmission loss data, the model is run at the nominal 1/3-octave band centre frequency, then averaged using a sliding range smoothing window on pressure magnitudes. This procedure (9) is fast and often employed in modelling of this type of data. For the synthetic cases, the model was run for a larger number of frequencies within each band, then averaged incoherently over each band. The second procedure is computationally slower but more correctly models this kind of data.

2.4.3 The Bartlett processor

For pressure field data recorded on an acoustic array, the incoherent broadband Bartlett processor is used. The processor is defined by

$$B(m) = \frac{1}{N_j} \frac{1}{M} \sum_{j=1}^{N_j} \sum_{k=1}^M \frac{\left| \sum_{i=1}^N d_{ijk}^* w_{ijk}(m) \right|^2}{\sum_{i=1}^N |d_{ijk}|^2 \sum_{i=1}^N |w_{ijk}(m)|^2} \quad (2.5)$$

² These settings were used when inverting data at 16-160 Hz to a range of 20 km.

with d the observed (complex) pressure and $w(m)$ the modelled pressure for model vector m . The inner summations (index i) are over N hydrophones of the array. The outer summations are over M frequencies (index k) and N_j arrays (index j). The summation over frequencies is incoherent, with equal weight to all frequency components. The processor takes values between zero and one with one indicating a perfect match. For use in inversion, an energy function $E(m)=1-B(m)$ is defined.

2.4.4 The TL processor

Three energy functions commonly used for transmission loss data are the average absolute error, the least squares error and the "TL processor". Here, the TL processor is used:

$$E_{TL}(m) = \sqrt{\frac{1}{N} \sum_{j=1}^N \left[-20 \log|d_j| - (-20) \log|w_j(m)| \right]^2} \quad (2.6)$$

with d the observed data, $w(m)$ is the synthetic pressure field for seabed model m , j a summation index over frequencies and ranges and N the total number of data points. Note that transmission loss on a logarithmic (dB) scale is used.

2.4.5 Model parameters

The source-receiver parameters (source depth, receiver depth and source-receiver ranges) were kept fixed at nominal values. This helped reduce computation effort in the use of the OASES forward model. For real data, nominal shot ranges were determined from the measured shot arrival time converted to range using a simple eigenray computation for a simplified environment; actual source depths were determined (and used in the estimation of source levels) by analysis of bubble pulse periods. The following geoacoustic model parameters were included in inversions:

- geoacoustic layer compressional (p-) wave velocity
- geoacoustic layer shear (s-) wave velocity
- geoacoustic layer density
- geoacoustic layer thickness.

For a two-layer seabed (sediment over halfspace) this yields a total of seven inversion parameters. The p- and s-wave attenuations were fixed at standard Hamilton values. For some inversions, a relation between the s- and p-wave velocity of a sediment layer was introduced using a standard velocity ratio of 0.50.

For each parameter, from sixteen to one hundred subdivisions of the search interval was used. With seven parameters and one hundred subdivisions of each parameter, the total size of the parameter space is 10^{14} . In some cases, the size was limited by using fewer subdivisions for less sensitive parameters and by keeping sets of parameters fixed or linked by interrelations.

There is an inherent interdependency of the shear and compressional wave velocities of elastic media, as both are related to the density of the medium via Lamé constants (e.g. Eqs. 4.30-4.31 in Ref 10). It is thus an issue whether both the shear speed and the density of a

geoacoustic layer can be estimated unambiguously at the same time. It is also noted that the p-wave attenuation and s-wave velocity may have a similar effect on propagation for a large class of problems. The issue of choice of inversion parameters for elastic seabeds has most recently been discussed in Ref. 11.

2.4.6 A posteriori statistics

Estimates of the model parameters and their statistical distributions are provided by SAGA. For a complete description of procedures, see Ref. 7. The estimated quantities are the mean,

$$\langle \mathbf{m} \rangle = \int \mathbf{m}' P(\mathbf{m}' | \mathbf{d}^{\text{OBS}}) d\mathbf{m}' \quad (2.7)$$

the one-dimensional marginal probability densities,

$$P(m_i | \mathbf{d}^{\text{OBS}}) = \int \delta(m_i' - m_i) P(\mathbf{m}' | \mathbf{d}^{\text{OBS}}) d\mathbf{m}' \quad (2.8)$$

and the parameter covariances

$$C_M = \int (\mathbf{m}' - \langle \mathbf{m}' \rangle)(\mathbf{m}' - \langle \mathbf{m}' \rangle)^T P(\mathbf{m}' | \mathbf{d}^{\text{OBS}}) d\mathbf{m}' \quad (2.9)$$

Here $P(\mathbf{m} | \mathbf{d}^{\text{OBS}})$ is the *a posteriori* probability density function of a model vector \mathbf{m} given observed data \mathbf{d}^{OBS} . The integrals in (2.7) and (2.9) extend over all parameter values of all elements of the model vector. In (2.8), the desired element m_i of the model vector is excluded from integration. The integrations should in principle extend over the entire parameter spaces, in practice the integrations have to be limited. In an earlier version of SAGA (version 3.1) the integrations were based on a selection of the best-fit members of the *last* generation of all populations. The samples are weighted according to the value of their energy function. The limited sampling has later been refined (SAGA version 4.1, Ref 7) to include use of all samples collected during the inversion. In the present work, for final model parameter estimates, the parameter values providing the maximum of the marginal a posteriori distribution for each parameter (as computed by SAGA-4.1) are used. These estimates are referred to as the *GA-max* estimates.

Execution times for a typical inversion run on a twin-processor HP-7000 series computer (processor speed 650 MHz) was 2 to 3 hrs per processor for a problem with two elastic seabed layers, constant sound speed and density profiles in all layers, the pressure fields computed by OASES for ten frequencies (16-160 Hz) to a range of 20 km, with 16,000 models evaluated.

3 SYNTHETIC DATA

Two types of seabed environments are studied: the soft elastic two-layer seabed test cases of the 1997 inversion workshop (3) and two thin-layer cases representative of anomalous Continental Shelf seabed environments (12,13). The Bartlett and transmission loss processors are applied to noise-free synthetic data. Inversions for geoaoustic model parameters are conducted using the genetic algorithm global search method of SAGA (7).

The transmission loss processor was first used in a simulation study by Heard et al. (4). They applied the TL and Bartlett processors to selected synthetic test cases, and found that the TL processor performed best when applied in 1/3-octave bands (the 32 Hz and 50 Hz bands were simulated separately) as opposed to a broad band (25-100 Hz), and better if results from different 1/3-octave bands were averaged (the authors do not state the averaging procedure), yet results were as expected inferior to those obtained using Bartlett processors. A genetic algorithm global search was used; model arrays in vertical and horizontal configurations were tested. For the same synthetic test cases, Vesterlin (see Ref 3) applied a variant of the TL processor in a global genetic algorithm inversion scheme. He used large amounts of data (many ranges and/or depths and many frequencies) to obtain good results, but also found that using a few narrowband frequencies provided results of equal quality. None of these authors applied the TL processor to the elastic seabed test cases. The elastic seabed test cases were addressed by Ratia et al (14) and Fallat and Dosso (16) using low-frequency multi-frequency VLA data with the Bartlett processor and global search algorithms, and by Knobles (15) using a large set of data in a non-linear least squares approach to inversion. Dosso et al (17) have later revisited the complete set of 1997 workshop test cases.

3.1 Test cases

The EL test cases (3) consist of a soft sediment layer of shear speed 100-300 m/s and thickness 30-80 m (maximum and minimum values provided) over a halfspace of shear speed 200-500 m/s. The geometry of the waveguide is: water depth 100 m, source depth 20 m, receiver arrays at ranges 1.0-5.0 km (horizontal arrays at depths 75 m and 100 m, ranges 0.05-5.0 km). Two additional test cases, labelled the CS test cases, have been designed to represent hard elastic seabed environments, based on seabed models used by Hovem et al. (13) for two Continental Shelf sites. The same waveguide geometry of water depth 100 m and maximum range 5 km has been used for these cases. For the test cases, noise-free synthetic data was generated using the OASES forward model. The synthetic data set was then "inverted" for a selected set of realistic experiment configurations and processors. In the inversions, water depth and source positions were fixed at true positions. The seven geoaoustic seabed parameters to be estimated were: p- and s- wave velocities and densities of the two sediment layers and the thickness of the sediment layer. Inversions were performed using the genetic algorithm global search method of SAGA. Search parameters intervals were provided with the test cases.

3.2 Experiment configurations

Two experiment configurations were tested for the incoherent broadband Bartlett processor: a 20-element vertical line array (VLA) at range of 1.0 km spanning the water column and a 20-element horizontal line array (HLA) of length 2000 m at the seabed at ranges 3.0-5.0 km, with spacing increasing from 50 m (five elements closest to source) to 100 m (next eleven elements) and 200 m (four elements farthest from source). The source depth was for these cases 20 m, endfire to the HLA. A standard set of three processing frequencies at 32 Hz, 63 Hz and 160 Hz was chosen for these configurations.

	Label	Sensor Range [km]	Sensor Depth [m]	Number of sensors	Sensor Spacing [m]	Processing Frequencies [Hz]	Processor Type
1	VLA	1.0	5-100	20	5.0	32,63,160	Bartlett
2	HLA	3.0-5.0	100	20	50-200	32,63,160	Bartlett
3	TL-O3	0.5-5.0	20	16	300	32,63,160	TL 1/3-octave
4	TL-O8	0.5-5.0	20	16	300	32-160	TL 1/3-octave
5	TL-nb	0.5-5.0	75	91	50	32,63,160	TL multi-tone

Table 3.1 Source-receiver configurations, processing frequencies and processor types used for the EL and CS test cases.

With the TL processor, the receiver positions constitute independent measurements, since there is no relative phase in the summations of the processor. By invoking the reciprocity principle, a HLA configuration for the TL processor can then alternatively be taken to represent a single receiver and sources at varying range. This configuration closely resembles the experiment configuration using SUS charges at increasing range from a single sensor in the water column.

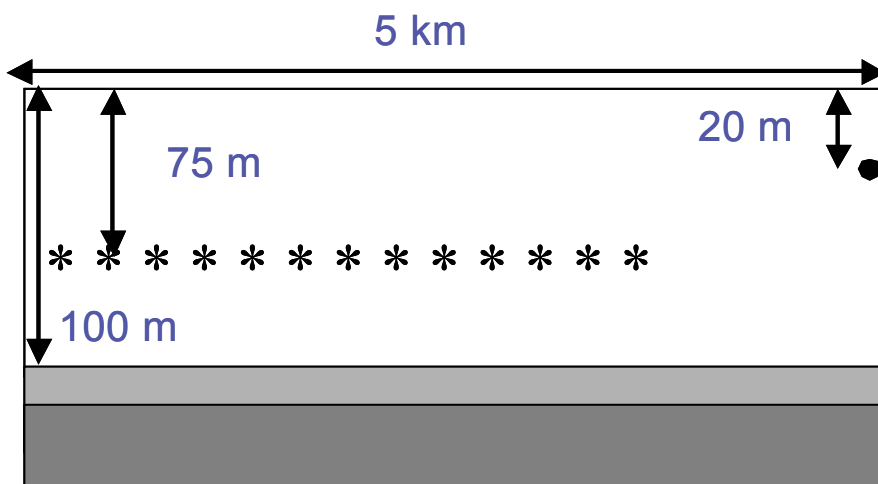


Figure 3.1 Test case geometry for configuration using the TL processor. Sources (stars) are at depth 75 m in a 100 m depth waveguide. A single receiving sensor (black dot) is at a depth of 20 m. Source ranges are up to 5.0 km.

The configurations were tested with data from two, three, four, eight and ten 1/3-octave frequency bands from 32-250 Hz. Results from use of three and eight frequency bands at 32-160 Hz will be shown; results for some additional configurations are tabulated in the

Appendix. The test case geometry for the TL processor is depicted in Figure 3.1. A sensor depth of 20 m and receiver depth of 75 m were selected as provided from the test case data.

A configuration representing a multi-tone source tow was also tested. This kind of data is often collected for area characterization (18). Both the TL processor and the average absolute error processor were applied (using data on a dB scale); results will only be presented for the former. Thus, a total of five experiment configurations will be reported in this chapter. The parameters of all configurations, frequencies and processor used, as listed in Table 3.1, were kept fixed for the entire study, after this initial choice had been made.

3.3 Presentation of results

Results will be compared to those obtained during the 1997 workshop (3). These were for the EL case by Ratial et al. (14) using data at 25 Hz and 199 Hz, a 100-element VLA at range 1.0 km, the OASES forward model, the incoherent broadband Bartlett processor and the genetic algorithm search method of SAGA, by Fallat and Dosso (15) using a simulated annealing search with data at 100 Hz for five 100-element VLA at ranges from 1 km to 5 km and by Knobles et al. (16) using a non-linear least squares inversion technique applied to data at 25-500 Hz for a variety of array configurations. Dosso et al. (17) have later refined their method and results for this and other test cases from the workshop, using the ASSA inversion method, data from a more realistic 20-element VLA at range 1.0 km and the Bartlett processor applied to data at 100 Hz. Results from (14), (16) and (17) will be used.

Results are summarized in terms of the mean absolute deviation error (MADE) of the parameter estimates, defined by

$$\text{MADE} = \frac{1}{M} \sum_{i=1}^M |y_i - \hat{y}_i| \quad (3.1)$$

with M the number of unknown parameters, y_i the i 'th true parameter value and \hat{y}_i the i 'th estimated parameter value. Both the true and estimated parameter values are normalized by the width of the search interval for the parameter (3). It should be noted that only for simulated data is a "true" parameter value available and MADE usable as a measure of inversion performance. In a complete analysis of inversion results, an uncertainty analysis must be a component. This important point is not further addressed here.

3.4 The EL cases

3.4.1 Seabed models

The seabed model for test case EL-A is shown in Table 3.2. It consists of a thick soft elastic sediment layer over a soft elastic halfspace, both of s -wave velocity less than 600 m/s. Both layers are homogeneous. There is a constant negative sound speed gradient (-20 m/s over 100 m) in water. The parameters in italics were inverted for and should be considered unknown prior to the inversion. Parameters for two similar test cases (cases EL-B and EL-C) are provided in the Appendix. The synthetic data set was downloaded from a workshop site.

Layer	Thickness [m]	P-wave velocity [m/s]	S-wave velocity [m/s]	P-wave attenuation [dB/ λ]	S-wave attenuation [dB/ λ]	Density [g/cm ³]
Water	100.0	1480/1460	-	-	-	1.00
Sediment	<i>55.1365</i>	<i>1669.35</i>	<i>130.630</i>	0.103397	0.25	<i>1.85324</i>
Halfspace		<i>1728.47</i>	<i>406.911</i>	0.087575	0.25	<i>2.06771</i>

Table 3.2 Geoacoustic environment for test case EL-A. Parameters in italics were included in the inversions.

3.4.2 Results

Inversions were run using SAGA-4.1 for a preset number of forward models (four independent populations, 2000 forward models evaluated for each population), with the OASES forward model. For TL data in 1/3-octave bands, the forward model was run for a number of frequencies within each band (spacing 1 Hz), then averaged incoherently³. This increased computation time to 26 hrs for runs when using data from eight frequency bands.

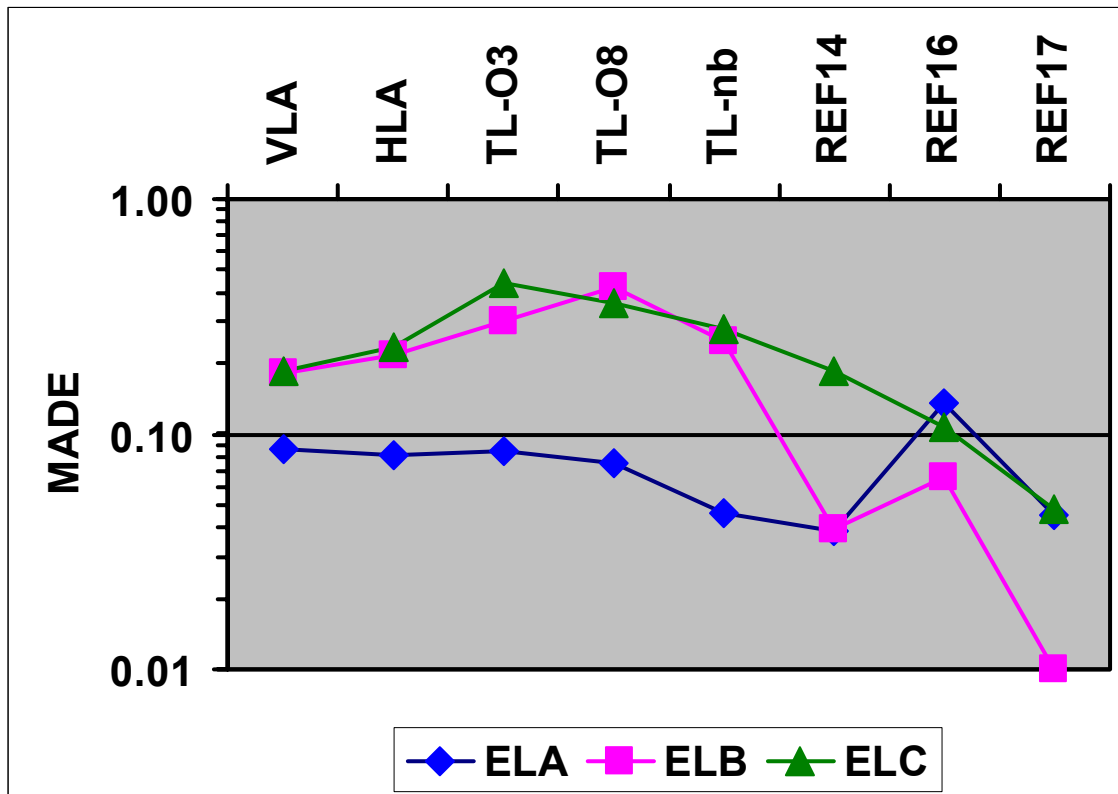


Figure 3.2 Mean absolute deviation error (MADE) in seabed geoacoustic parameter estimates from inversion for EL test cases from the Inversion Workshop 1997. Five experiment configurations (Table 3.1), three results by others.

Figure 3.2 shows the results obtained in terms of the MADE for the three EL test cases using the five experiment configurations. Three results obtained by others are also included in the

³ This is a local addition to the SAGA code. For frequency bands up to 100 Hz, a spacing of 1 Hz was used; for bands 125 Hz and 160 Hz a spacing of 2 Hz; for frequencies above a spacing of 5 Hz.

Figure for comparison. The configurations and labels of the vertical axis is as follows: VLA and HLA Bartlett (1-2), TL 1/3-octave (3-4), TL multi-tone (5) and results obtained by others (6-8). For the workshop (3), results with a MADE less than 0.10 were considered *excellent*. For those three research groups who addressed the EL test cases, one group met this criterion in all three cases and two in two of three cases. In the present study, *excellent* results as measured in terms of the MADE have been achieved only for the EL-A test case. *Good* results (a MADE of 0.20 or less) have been achieved for the EL-B and EL-C test cases using complex pressure data and the Bartlett processor for VLA data.

With the Bartlett processor, results both for VLA and for HLA data are comparable to those obtained by others for case EL-A. For case EL-B with a thicker sediment layer (75.6 m as opposed to 55.1 m for case EL-A), results are inferior to all references. Inclusion of data at additional low frequencies or a different weighting of low-frequency data could presumably improve results. For case EL-C (sediment thickness 34.8 m) results for the Bartlett processor are comparable to those of Ref 14. The results shown are representative of a wider variety of configurations tested for the Bartlett processor. Additional results using a HLA at shorter range (1.0-3.0 km) are tabulated in the appendix.

The configurations using the TL processor perform comparable to those using the Bartlett processor only for the EL-A test case. Use of three frequency bands (32 Hz, 63 Hz and 160 Hz) performs as well as use of all eight bands within the interval 32-160 Hz. Comparable results were obtained using two bands (32 Hz and 63 Hz) and ten bands at 25-200 Hz (see the Appendix for details). As demonstrated in the next section, the TL processor tended to find a s-wave velocity of sediment at the upper bound of the search interval (300 m/s) and a wrong value of s-wave velocity of the halfspace. Thus the average s-wave velocity is close to correct whereas the values of each medium as used in the MADE are far from the true values. Also, estimates of densities are poor, contributing to a high MADE. The use of an alternative set of inversion parameters for the EL-B test case has been discussed in Ref. 18.

Use of multi-tone data with the TL processor performs overall slightly better than use of TL data processed in 1/3-octave bands. Marginally better results could be obtained by use of other sets of frequencies. Additional results using the TL processor with narrowband data are tabulated in the Appendix.

3.4.3 Parameter estimates

Tables of true and estimated parameter values of all seven inversion parameters for all configurations and all three EL test cases are provided in the Appendix. Scatter plots of individual parameter estimates by five configurations for two combinations of parameters are shown in Figure 3.3 (p-wave velocities) and 3.4 (s-wave velocities).

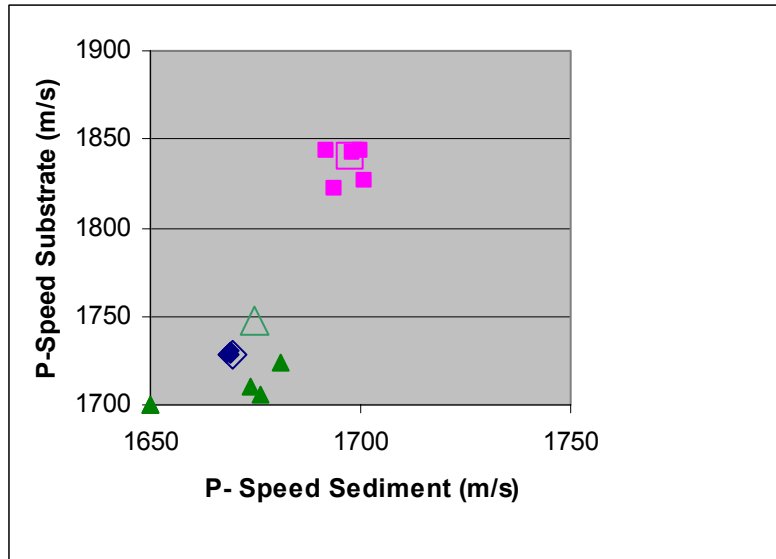


Figure 3.3 Scatter plot of estimates of *p*-wave velocities in sediment (*x*-axis) and substrate (*y*-axis) from inversion for configurations 1-5 for the three EL test cases. Open markers indicate true parameter values. Axis limits indicate parameter search intervals. The cases are EL-A (blue diamonds), EL-B (pink squares) and EL-C (green triangles).

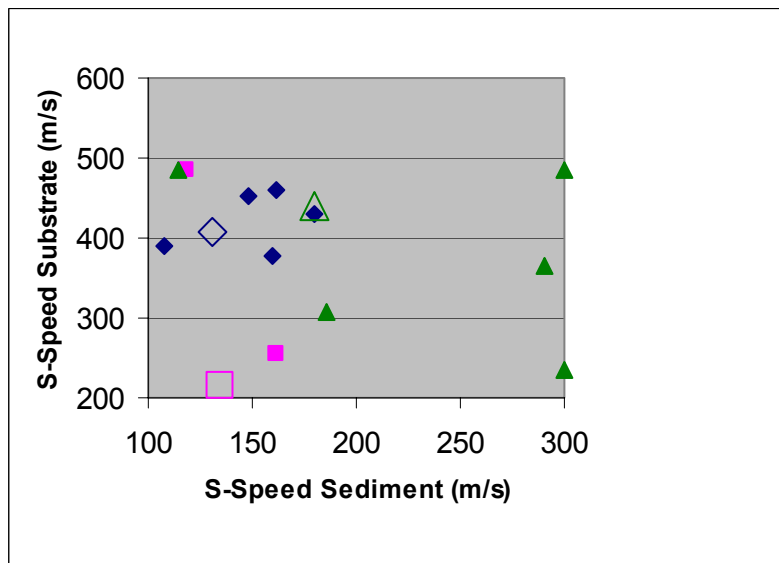


Figure 3.4 Scatter plot of estimates of *s*-wave velocities in sediment (*x*-axis) and substrate (*y*-axis) from inversion for configurations 1-5 for the three EL test cases. Open markers indicate true parameter values. Axis limits indicate parameter search intervals. The cases are EL-A (blue diamonds), EL-B (pink squares) and EL-C (green triangles).

The overall best estimated parameters were the sediment thickness (not shown) and the *p*-wave velocities of the sediment and halfspace. Poor estimates are noted for the densities and *s*-wave velocity of the sediment and halfspace (except for case EL-A).

3.5 The CS cases

Additional test cases were designed from a series of seabed models used by Hovem et al. (13) to model two anomalous Continental Shelf seabed environments⁴. The same waveguide geometry as for the EL test cases was used. For simplicity the sound speed in water was here set to a constant value of 1470 m/s. The two test case seabed models labelled CS-B and CS-D are listed in Tables 3.3 and 3.4 respectively. The synthetic data was generated at FFI using the OASES forward model in stand-alone mode. The complex pressure fields were computed in 1 Hz increments from 20 Hz to 180 Hz and in 2 Hz increments from 182 Hz to 280 Hz. Parameter search bounds were set up as listed in the Appendix.

3.5.1 Seabed models

Test case CS-B consists of a thin shear-supporting sediment layer over a hard elastic substrate of s-wave velocity 1900 m/s and p-wave velocity of 4700 m/s. Parameters of the model are listed in Table 3.3.

Test case CS-D consists of a shear-supporting sediment layer over a hard elastic halfspace of s-wave velocity 2200 m/s and p-wave velocity of 4700 m/s. Parameters are listed in Table 3.4. Two additional seabed models with fluid sediment layers were also designed in (13); these are not considered further here.

Layer	Thickness [m]	P-wave velocity [m/s]	S-wave velocity [m/s]	P-wave attenuation [dB/λ]	S-wave attenuation [dB/λ]	Density [g/cm ³]
Water	100	1470	-	-	-	1.00
Sediment	<i>2.00</i>	<i>1700</i>	<i>200</i>	<i>0.50</i>	<i>0.50</i>	<i>1.80</i>
Halfspace		<i>4700</i>	<i>1900</i>	<i>0.10</i>	<i>0.10</i>	<i>2.40</i>

Table 3.3 Geoacoustic environment for test case CS-B. Parameters in italics were included in the inversions.

Layer	Thickness [m]	P-wave velocity [m/s]	S-wave velocity [m/s]	P-wave attenuation [dB/λ]	S-wave attenuation [dB/λ]	Density [g/cm ³]
Water	100	1470	-	-	-	1.00
Sediment	<i>10.00</i>	<i>1700</i>	<i>200</i>	<i>0.50</i>	<i>0.50</i>	<i>1.80</i>
Halfspace		<i>4700</i>	<i>2200</i>	<i>0.10</i>	<i>0.10</i>	<i>2.40</i>

Table 3.4 Geoacoustic environment for test case CS-D. Parameters in italics were included in the inversions.

Attenuations (p- and s-wave) were fixed also for these inversions, at values somewhat lower than those used in (13). All layers of the models were homogeneous.

⁴ Siedenburg et al (Ref 19) devised a set of three noisy synthetic test cases with a thick elastic sediment layer over an elastic halfspace. One of their cases consisted of a 58 m thick sediment over hard elastic halfspace.

The CS cases constitute a different class of models than the EL cases in that particular shear-dependent wave types can be excited in the seabed and affect the propagation conditions. The CS seabed models can cause high propagation loss at below-critical grazing angles due to two particular effects:

- guided shear waves in the sediment (cases CS-B and CS-D)
- interface waves at the sediment-substrate boundary (case CS-D only).

A quick glance at expected propagation conditions for these types of seabed environments can be obtained from the plane-wave reflection coefficients at the water-seabed interface. These have been computed (using the OASR module of OASES) for the seabed models EL-A and CS-D and plotted in Figure 3.5. (See also Ref. 13 for plots of model CS-B.)

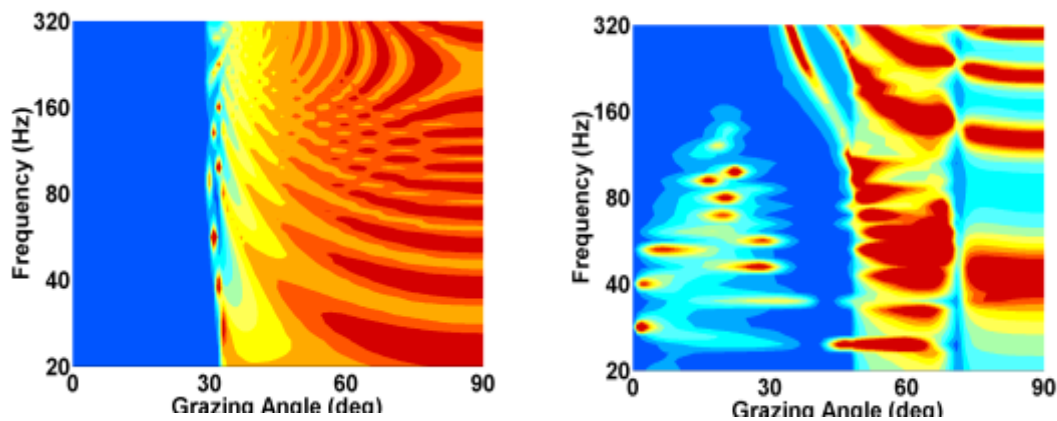


Figure 3.5 Plane-wave reflection loss (dB) versus grazing angle and frequency for two elastic seabed models. Case EL-A (left panel) and CS-D (right panel). Dynamic range 0 dB (blue) to 10 dB (red).

Case EL-A exemplifies the EL cases: there is a well-defined p-p critical angle (at about 29° for case EL-A) and no p-s critical angles. The p-p critical angle varies only slightly with frequency. Good propagation conditions are expected. For case CS-D (and case CS-B, not shown), a sequence of distinct high-loss bands appears for discrete frequencies at grazing angles below p-p critical (at about 30°). The bands, their origin and association with guided shear waves in the sediment are further discussed in Refs 12 and 13. For case CS-D there is in addition a broad region in frequency and grazing angles of high loss at about 25 Hz to 160 Hz. This is associated with the excitation of interface waves at the sediment-substrate boundary, as further discussed in these references. Effects of both loss mechanisms have been observed in broadband transmission loss data acquired at the Continental Shelf (12).

3.5.2 Results

Results measured by the MADE for the five configurations for test cases CS-B and CS-D are shown in Figure 3.6. For these cases, there is (as yet) no comparison with results by others.

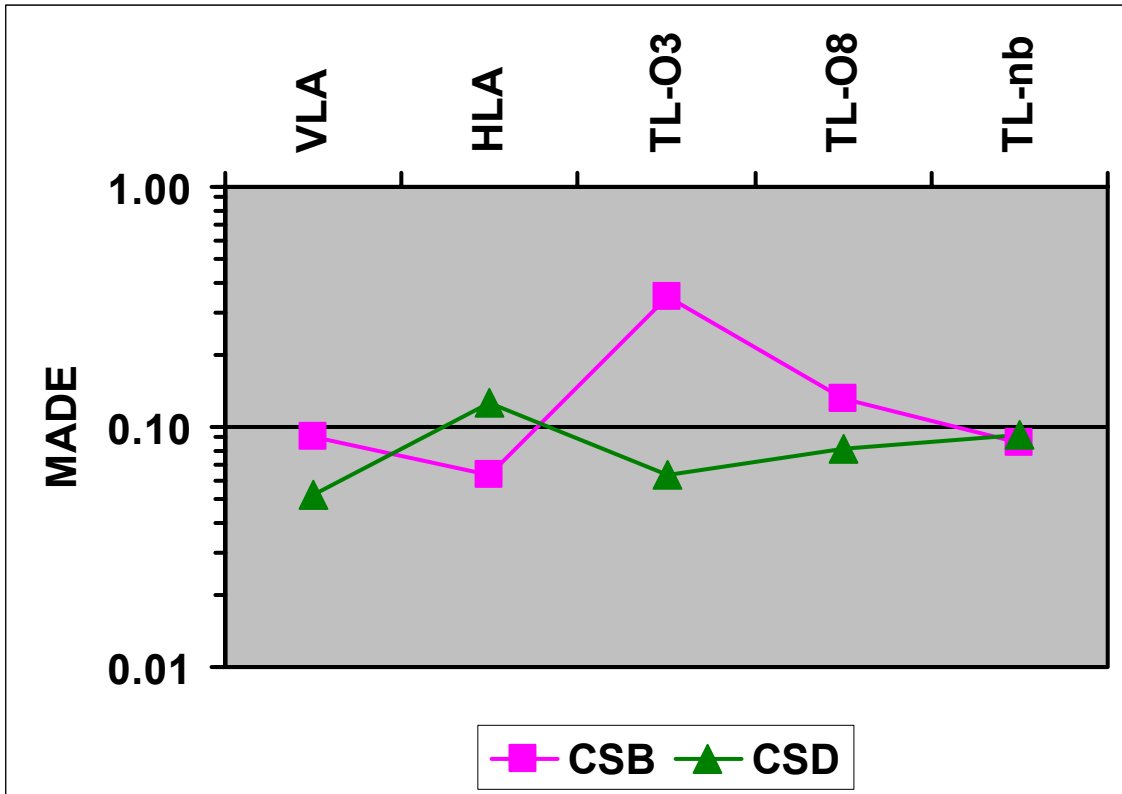


Figure 3.6 Mean absolute deviation error (MADE) in seabed geoaoustic parameter estimates from inversion for test cases EL-A, CS-B and CS-D. Five experiment configurations.

The MADE achieved for these test cases is overall slightly higher than that achieved for the EL-A test case. *Excellent* results (a MADE of 0.10 or less) have been obtained for case CS-B using the Bartlett processor with VLA and HLA data and for case CS-D using the Bartlett processor with VLA data and using the TL processor. The TL processor using eight frequency bands gives a *good* result also for case CS-B. In summary, best overall results have been obtained using the Bartlett processor with VLA data and with the TL processor with *many frequency bands*. Results for some additional configurations are listed in the Appendix.

3.5.3 Parameter estimates

Individual parameter estimates are plotted in Figure 3.7 for the combination of s-wave speed in sediment and sediment thickness, and in Figure 3.8 for the combination of s-wave speed in substrate and p-wave speed in sediment. Further results for all parameter estimates are tabulated in the Appendix.

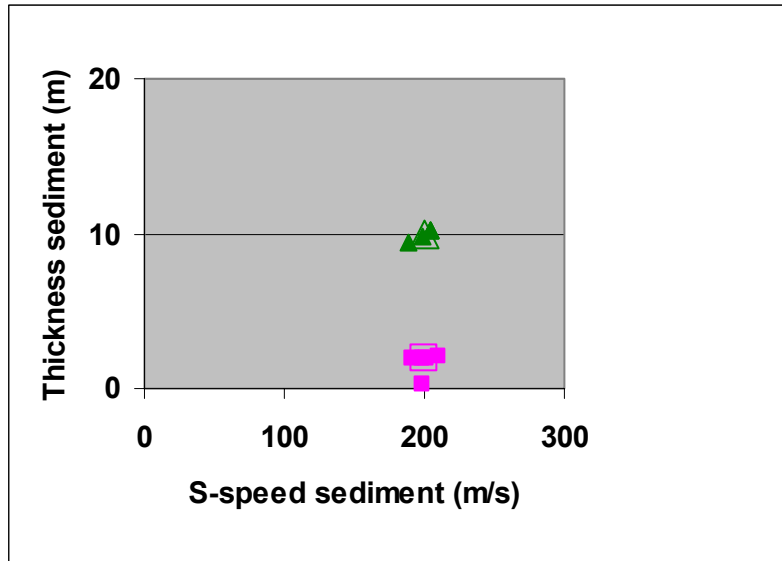


Figure 3.7 Scatter plot of estimates of s -wave velocity in sediment (x -axis) and thickness of sediment (y -axis) from inversion for configurations 1-5 for the two CS test cases. Open markers indicate true parameter values. Axis limits indicate search intervals. Case CS-B (pink squares) and CS-D (green triangles).

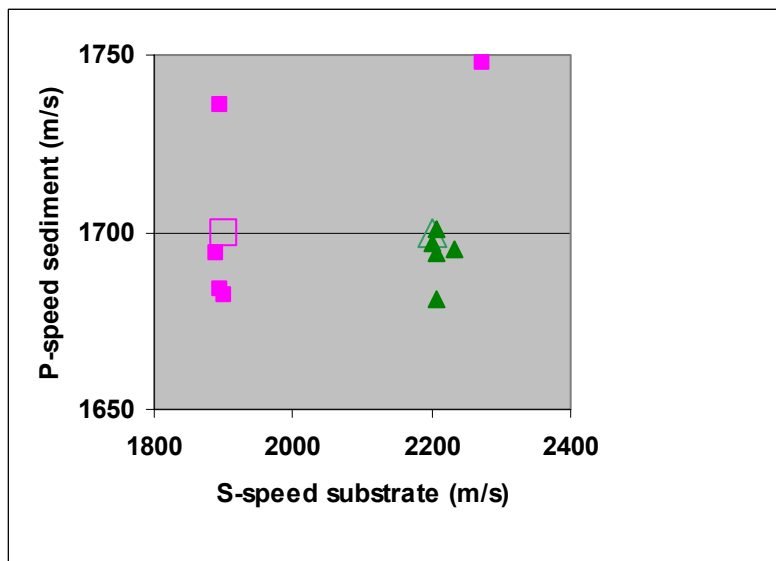


Figure 3.8 Scatter plot of estimates of s -wave velocity in substrate (x -axis) and p -wave velocity of sediment (y -axis) from inversion for configurations 1-5 for the two CS test cases. Open markers indicate true parameter values. Axis limits indicate search intervals. Case CS-B (pink squares) and CS-D (green triangles).

By a not-so-rigorous judgement, the ability of the TL processor to estimate the individual parameters can be categorized as such:

- sediment s -wave speed and thickness: excellent
- sediment p -wave speed: mixed
- substrate s -wave speed: excellent
- substrate p -wave speed and densities: poor.

One may be surprised to find that s -wave parameters are better estimated than p -wave parameters for these cases. A clue to this is seen in the plots of reflection coefficients for

these two environments. It is seen that the p-p critical angles are “masked” by additional loss for lower-than-grazing angles and the first apparent critical angle at low frequencies is p-s conversion at the sediment-halfspace interface. Thus mechanisms sensitive to p-wave velocities only are not probed as direct as for the EL cases. A finer tuning of use of frequencies, as could be accomplished by an inspection of all acoustic data prior to selection of data for use in inversion, presumably would improve results in this respect.

The combination of parameters selected for presentation on Figures 3.7 and 3.8 are the combinations essential to the two loss mechanisms present in test cases CS-B and CS-D. The parameter sensitivities are not similar for these two mechanisms. Although individual parameter estimates from inversion are not necessarily correct, their *combinations causing high propagation loss* have in *both* cases been well predicted using the TL processor. This may be an important result for practical applications.

3.6 Geometric parameters

The question of robustness to mismatch in source depth and water depth is addressed. In the test cases considered above, these parameters as well as source ranges and receiver depths were fixed. These geometric parameters are often determined to good accuracy in an acoustic experiment. To check the robustness of the Transmission Loss processor to errors in water depth and source depth, a sensitivity analysis has been done for configurations 3 and 5 of Table 3.1. A study is conducted by varying the parameter value over a defined interval, computing the processor output at each value, keeping other parameters fixed at nominal.

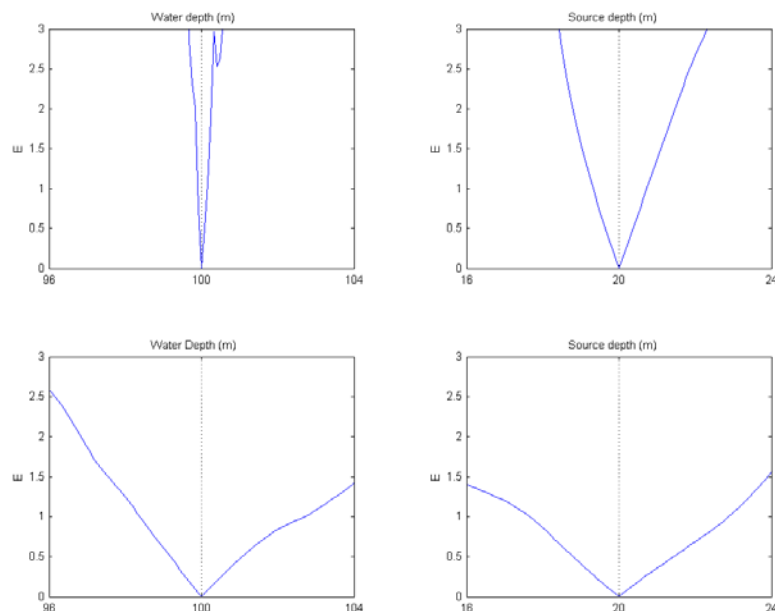


Figure 3.9 Sensitivity to error in water depth (left panels) and source depth (right panels) using the TL processor with narrowband data (upper panels) and 1/3-octave band data (lower panels) at frequencies of 32 Hz, 63 Hz and 160 Hz combined. Vertical axis is TL processor output in dB.

Plots of processor output versus parameter value give a visual indication of parameter sensitivity. Figure 3.9 shows the results for the EL-A test case, using narrowband data (upper panels) and broadband data (lower panels) at 32 Hz, 63 Hz and 160 Hz combined. The figure illustrates the improved robustness of the TL processor using 1/3-octave band frequency averaged data over the use of narrowband data. Sensitivity to offset in range to individual sources has not been addressed.

3.7 Summary

A geoacoustic inversion study using noise-free synthetic data in a range-independent waveguide with a two-layer elastic seabed of unknown geoacoustic parameters has been conducted. Specific attention has been put to the use of broadband transmission loss data. It has been found that:

- the Bartlett processor applied to complex pressure data recorded at a VLA at short range will perform best in all cases,
- the Bartlett processor with a long HLA at the seabed (sources at endfire direction) will perform almost as good as a VLA in most cases,
- with broadband transmission loss data from several sources over range and a single hydrophone receiver, *key* seabed parameters can be recovered,
- with TL data, the use of data from *many* frequency bands is an advantage,
- for thin-layer hard-elastic seabed environments, estimates of key parameter *combinations* causing high propagation loss can be obtained; it is indicated that use of TL data may be an *advantage* for such environments.

Inversion for geoacoustic parameters in the environments considered is not a trivial task; these are challenging parameter spaces with many correlated parameters. The use of an inversion scheme based on genetic algorithms (SAGA) may have been an advantage in this respect. More realistic studies should eventually be repeated using data with added noise and other contributors to mismatch.

4 CONTINENTAL SHELF DATA

Sensitivity of transmission loss data to seabed model parameters in a Continental Shelf setting is briefly studied (section 2), then transmission loss data collected at two sites is used for geoaoustic inversion (sections 3 and 4).

4.1 Geometry

The Continental Shelf encompasses areas of water depths from 50 m at shallow banks increasing to 350 m or more in deeper basins and troughs. In the following, data collected at water depths 320 m – 350 m will be considered. Geometric parameters of the transmission loss data sets acquired on the Continental Shelf are listed in Table 4.1: water depth 350 m, source depth 91 m, maximum range 20 km.

	Water Depth [m]	Source Depth [m]	Processing Frequencies [Hz]	Ranges [km]
Test Cases	100	20	32-250	0.5-5.0
Continental Shelf	350	90	16-160	3.5-20

Table 4.1 Waveguide geometry parameters for synthetic test cases (second row) and for Transmission Loss data acquired at Continental Shelf (third row).

The geometry of the test cases considered for the synthetic study of Chapter 3 is also shown in Table 4.1. A crude comparison shows that these test cases can be considered as "scaled-down" versions of the geometry encountered in parts of the Continental Shelf and the acoustic experiments conducted therein.

A wide variety of seabed conditions are encountered at the Shelf. These range from soft elastic seabed types with thick (20-100 m) deposits of Quaternary sediment to anomalous thin-layer environments (sediment thickness 2-10 m) of the types exemplified in the previous chapter. Data from one of each of these types of seabed will be considered. To get insight into what to expect from the use of transmission loss data for inversion, parameter sensitivity is addressed for a soft type seabed.

4.2 Sensitivity study

The Continental Shelf geometry with a water depth of 350 m and data to a range of 20 km (parameters in the third row of Table 4.1) is used. The geoaoustic model is shown in Table 4.2 and represents a Continental Shelf environment of a soft seabed type.

Sensitivity of acoustic data to seabed geoacoustic parameters is studied for two configurations:

- Complex pressure field data recorded on a 26-element VLA spanning the lower portion of the water column (phone depths 100-350m, element spacing 10 m), a low-frequency broadband source at depth 90 m and range 3.5 km, processed at four frequency components (16 Hz, 32 Hz, 63 Hz and 125 Hz), incoherent broadband Bartlett processor.
- Transmission Loss data recorded at a single hydrophone at 90 m depth, sources at depth 90 m and ranges from 3.5 to 17.5 km at 1.5 km intervals, data processed in eleven 1/3-octave frequency bands (16 Hz - 160 Hz), transmission loss processor.

The first of these is a typical situation that would be used for geoacoustic inversion where the nearfield is exploited to achieve a higher sensitivity to seabed parameters. The second configuration resembles that used for collection of transmission loss data.

Synthetic data was generated using the OASES model. Gaussian noise was added to the complex pressure fields with a signal-to-noise ratio of +6 dB per phone. The same SNR is for simplicity used for sources at all ranges and at all frequencies. In modelling of 1/3-octave frequency band averaged data, single frequency modelling with subsequent sliding-range averaging was used, again for simplicity.

Layer	Thickness [m]	P-wave velocity [m/s]	S-wave velocity [m/s]	P-wave attenuation [dB/λ]	S-wave attenuation [dB/λ]	Density [g/cm ³]
Water	350	1471 top 1469 bot	-	-	-	1.00
Sediment 1	<i>80</i>	<i>1700</i>	<i>200</i>	0.40	0.40	1.80
Sediment 2	<i>120</i>	<i>2400</i>	<i>1200</i>	0.10	0.10	2.20
Substrate		<i>4000</i>	<i>2000</i>	0.10	0.10	2.40

Table 4.2 Geoacoustic environment for the Continental Shelf site sensitivity study. Sensitivity to eight seabed parameters in italics studied.

The sensitivity to the eight seabed parameters listed in italics is plotted in Figures 4.1 and 4.2. The plots are generated by keeping all but one seabed parameter fixed to nominal value, then computing the value of the processor for a range of values of the given parameter around nominal. For the Bartlett processor $10\log(1-B(m))$ in dB is plotted. For the TL processor, the processor output in dB is plotted (note that these measures are not directly comparable in magnitude). The parameters are layer p-wave velocity (left panels), s-wave velocity (middle panels) and layer thickness (right panels) for the first two sediment layers (upper and middle panels) and for the halfspace (lower panels). A dotted vertical line in each frame indicates the nominal parameter value.

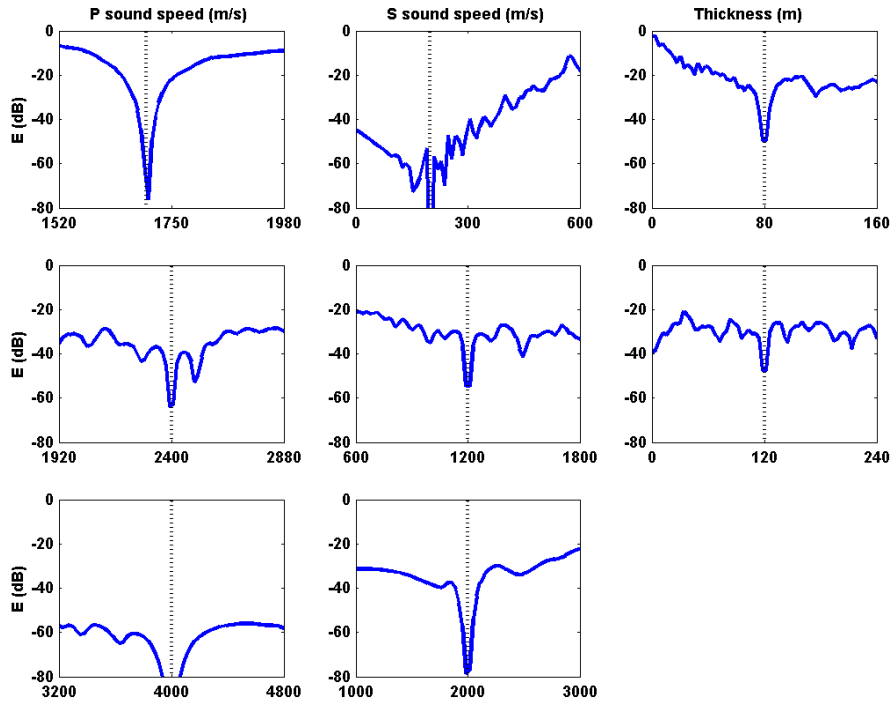


Figure 4.1 Parameter sensitivities using pressure field data (26-element VLA), incoherent broadband Bartlett processor, source at range 3.5 km, frequencies 16, 32, 63 and 125 Hz. Synthetic data; SNR +6 dB. Three-layer elastic seabed model.

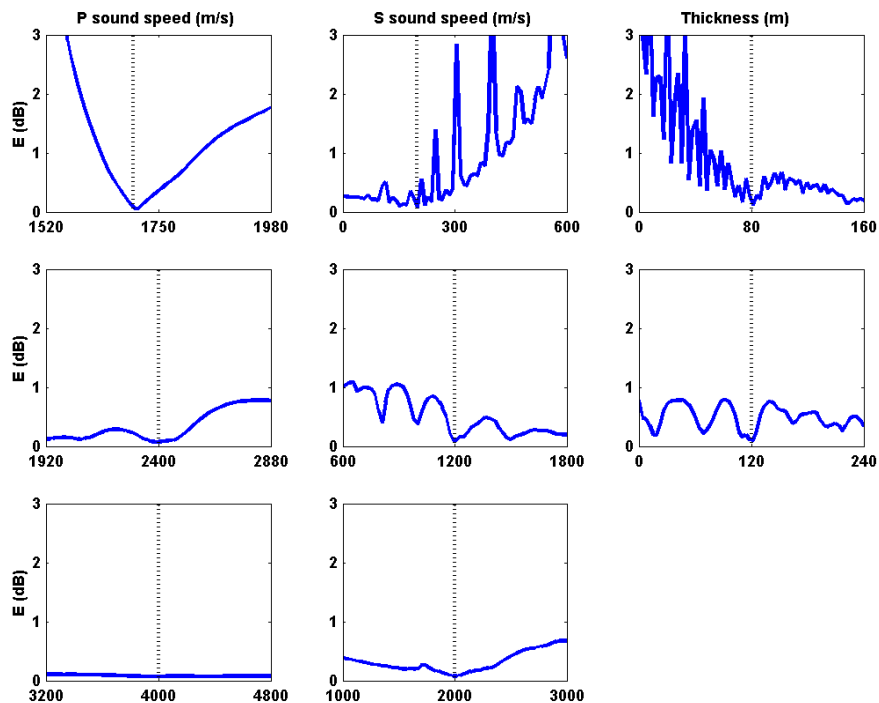


Figure 4.2 Parameter sensitivities using transmission loss data (single hydrophone), TL processor, source ranges 3.5-17.5 km, 1/3-octave frequency bands 16, 32, 63 and 125 Hz. Synthetic data; SNR +6 dB. Three-layer elastic seabed model.

It is observed that the VLA with pressure field data using the Bartlett processor has sensitivity to all parameters of all seabed layers. Using the TL processor, there is strong sensitivity to the p-wave velocity of the first sediment layer, some sensitivity to the thickness and s-wave velocity of the first seabed layer and to parameters of the second layer while sensitivity to parameters of the halfspace is lost. Comparable sensitivities were obtained using the TL processor with data from a 6-element VLA (results not shown).

Sensitivity to geometric parameters is addressed next. These parameters include source depth, water depth, receiver depth, array element positions and source-receiver ranges. Sensitivities to the first two are plotted in Figure 4.3.

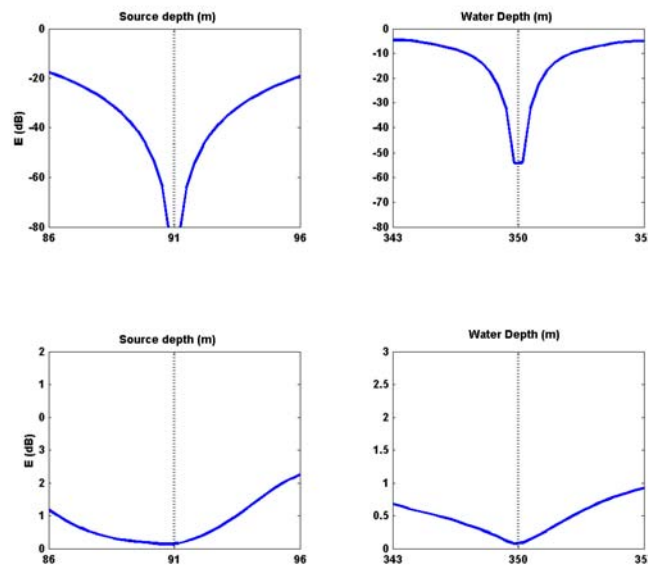


Figure 4.3 Sensitivity of processor output to mismatch in source depth (left panels) and water depth (right panels) for two experiment configurations: 26-element VLA with Bartlett processor (upper) and TL-data (lower). Synthetic data, SNR 6 dB.

A higher sensitivity to these geometric parameters is indicated for the configuration using the VLA and Bartlett processor, while the TL processor (broadband data) shows less sensitivity.

This sensitivity study indicates that configurations using VLA data and the Bartlett processor are preferential when estimates of geoaoustic parameter are desired, though these configurations are also more sensitive to geometric parameters. The transmission loss processor with broadband data is in general less sensitive to seabed geoaoustic parameters; it is also less sensitive to geometric parameters. The observations regarding sensitivity to seabed parameters are in agreement with those of the model study in the previous chapter.

4.3 Inversion setup

Two sets of transmission loss data (third-octave frequency band averaged) collected at the Continental Shelf are used for geoacoustic inversion. The data sets and collection will not be described in further detail. The inversion method has been described in detail in Chapter 2. Inversions were done using the genetic algorithm search method of SAGA (7). Four independent populations were run, testing a total of 32,000 models. The OASES forward model was used. Third-octave band averaged transmission loss was approximated by a range-average of pressure fields computed at the band centre frequencies. The transmission loss processor was used. Each inversion took approximately 4 hrs 30 minutes on a HP-7000 series computer using two processors. All parameter estimates quoted are the *GA-max* estimates obtained using all evaluated models.

4.4 Site S02

4.4.1 Baseline model

Acoustic data was collected to 20 km over a fairly range-independent layered seabed. The sound speed in water was nearly constant at 1470 m/s. Water depth changed from 355 m at the receiver site to 330 m at 20 km with a geometric mean water depth of 345.7 m. An interpretation of a seismic section collected along the acoustic track has produced the following baseline model: subcrop beneath Quaternary sediment is Triassic with an estimated p-wave velocity of 2.4 km/s, based on geophysical measurements of this geological unit from a nearby site. Beneath this is a stack of Perm-Carbon age layers. Estimates of properties of these layers are also from measurements of these units from a nearby site.

The range-independent baseline model of Table 4.3 is assumed. Properties of the Quaternary sediment layer are standard values for the Barents Sea and not related to in situ measurement at this or nearby sites. Shear wave velocities have been assigned using a s- to p- wave velocity ratio of 0.50.

Layer Type	Thickness [m]	P-wave velocity [m/s]	S-wave velocity [m/s]	P-wave attenuation [dB/λ]	S-wave attenuation [dB/λ]	Density [g/cm ³]
Water	350	1470	-	-	-	1.00
Quaternary	80	1800	300	0.50	0.50	1.80
Triassic	120	2400	1200	0.10	0.10	2.20
Perm- Carbon		4000	2000	0.10	0.10	2.40

Table 4.3 Baseline geoacoustic model for site S02.

Eleven parameters were included in the inversion: water depth, thickness of two sediment layers, all five geoacoustic parameters of the first sediment layer and three geoacoustic parameters of the second sediment layer. The parameters of the halfspace were fixed to baseline values. Note that several low-sensitivity parameters (as assessed by the study in

section 4.2) have been included in the inversion. Sound speed in water was set to a nominal value. The parameters included in the inversion, the baseline values and the parameter search intervals are listed in Table 4.4.

Parameter	Unit	Baseline Value	Search Interval	Steps
Water depth	m	350	343-357	32
Sediment 1 thickness	m	80	0-160	128
Sediment 1 p-velocity	m/s	1800	1520-1980	128
Sediment 1 s-velocity	m/s	300	0-600	128
Sediment 1 p-attenuation	dB/ λ	0.50	0.40-1.20	32
Sediment 1 s-attenuation	dB/ λ	0.50	0.40-1.20	32
Sediment 1 density	g/cm ³	1.80	1.64-2.26	32
Sediment 2 thickness	m	120	0-240	64
Sediment 2 p-velocity	m/s	2400	1920-2880	128
Sediment 2 s-velocity	m/s	1200	600-1800	128
Sediment 2 density	g/cm ³	2.20	1.98-2.42	16

Table 4.4 Inversion parameters for the site S02 model, baseline model values, search intervals and number of discretization steps.

The number of subdivisions of the search interval (equal size steps) was set to sixteen for less sensitive parameters and 128 for parameters of higher sensitivity. The total size of the search space was 10^{17} . Data from eleven frequency bands (16 Hz-160 Hz) and 19 ranges (1.5-20 km), a total of 209 data points, was used in the inversions.

4.4.2 Inversion results

Layer	Thickness [m]	P-wave velocity [m/s]	S-wave velocity [m/s]	P-wave attenuation [dB/ λ]	S-wave attenuation [dB/ λ]	Density [g/cm ³]
Water	<i>343.9</i>	1470		-	-	1.00
Sediment 1	<i>51</i>	<i>1610</i>	<i>70</i>	<i>0.71</i>	<i>0.40*</i>	<i>1.98</i>
Sediment 2	<i>167</i>	<i>2275</i>	<i>1384</i>	0.10	0.10	<i>2.42*</i>
Halfspace		4000	2000	0.10	0.10	2.40

Table 4.5 Geoacoustic model from inversion of transmission loss data at site S02. Parameters in italics were included in the inversion; other parameters were fixed to nominal. A star (*) indicates estimate at limit of search interval.

The model obtained from inversion (GA-max estimates) is shown in Table 4.5. The match with data (RMS error in dB averaged over all frequency bands) improved from 2.31 dB for the baseline model to 1.47 dB for the inversion model. Measured and modelled transmission loss is plotted in Figure 4.4 for all eleven frequency bands from 16 Hz to 160 Hz. The per-parameter one-dimensional marginal a posteriori probability distributions for the model parameters are plotted in Figure 4.5.

The parameters, baseline values, estimated values and standard deviations⁵ are listed in Table 4.6. The magnitude of the correlation coefficients between the inversion parameters is plotted in a matrix in Figure 4.6. The best-estimated parameters as judged by low standard deviations are the water depth, thickness of the sediment layers, the p-wave velocity of the first sediment layer and the p- and s-wave velocity of the second sediment layer. These are recognized to be the most sensitive parameters as judged by the model sensitivity study of section 4.2. The poorest estimated parameters are the layer densities and the s-wave velocity and attenuations of the first sediment layer. The most strongly correlated parameters are: the s-velocity and p-attenuation of the first seabed layer and the s-velocity and thickness of the second seabed layer. These correlations both have physical explanations that have been commented on in previous sections.

Parameter	Unit	Baseline	Inversion Estimate	Standard Deviation
Water depth	m	350	343.9	<0.001
Sediment 1 thickness	m	80	51.6	<0.001
Sediment 1 p-velocity	m/s	1800	1610	0.003
Sediment 1 s-velocity	m/s	300	70	0.005
Sediment 1 p-attenuation	dB/ λ	0.50	0.71	0.005
Sediment 1 s-attenuation	dB/ λ	0.50	0.40	0.090
Sediment 1 density	g/cm ³	1.80	1.98	0.028
Sediment 2 thickness	m	120	167	<0.001
Sediment 2 p-velocity	m/s	2400	2275	0.001
Sediment 2 s-velocity	m/s	1200	1384	<0.001
Sediment 2 density	g/cm ³	2.20	2.42	0.115

Table 4.6 Model parameters at S02: baseline values, estimated by inversion of transmission loss data, and normalised standard deviation of estimates.

⁵ The standard deviations are normalised by their search intervals. A flat distribution would have a value of 0.29; a distribution that is flat in half of the search interval would have a value of 0.10 for this quantity (10).

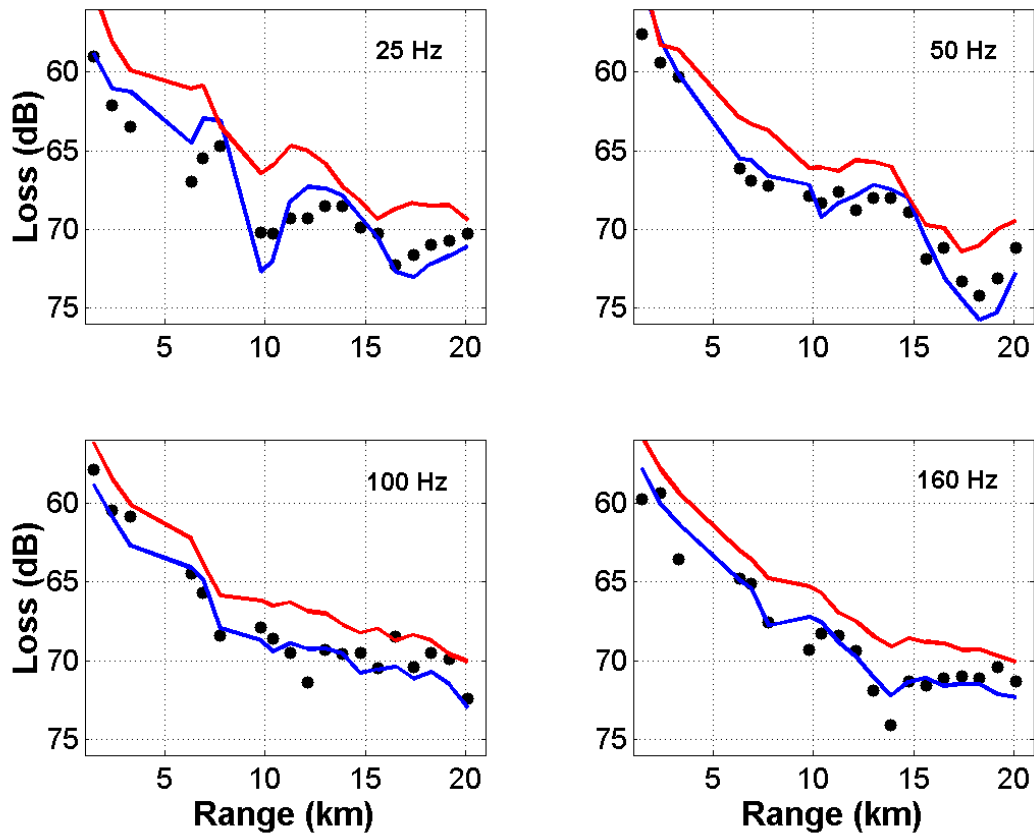


Figure 4.4 Measured and modelled transmission loss (dB) versus range (km) at site S02. Frequencies 25 Hz, 50 Hz, 100 Hz and 160 Hz. Data (black dots), modelled loss using geoacoustic model from inversion (blue line) and baseline geoacoustic model (red line).

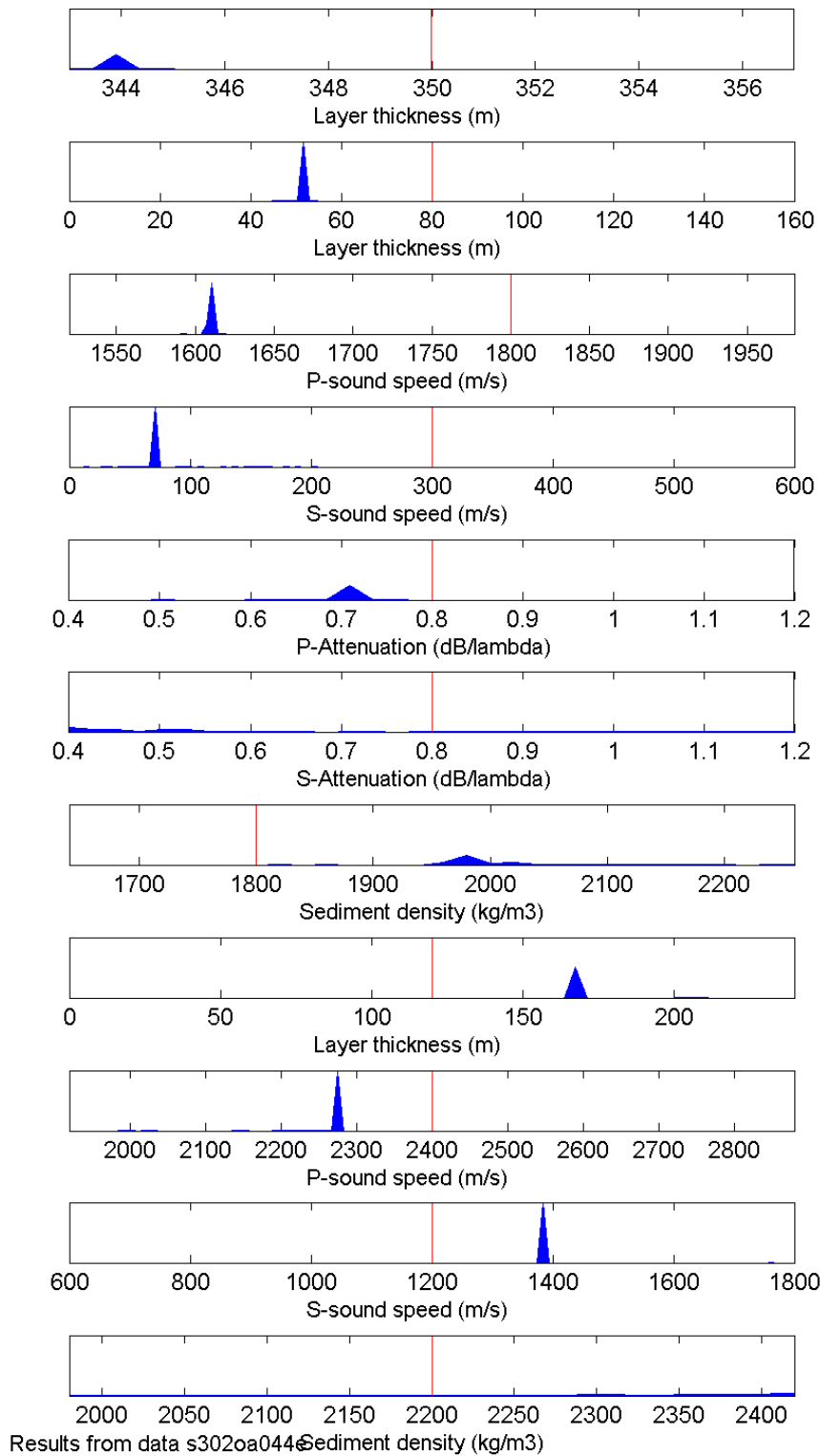


Figure 4.5 Marginal a posteriori probability densities for inversion parameters at site S02, as estimated by SAGA.

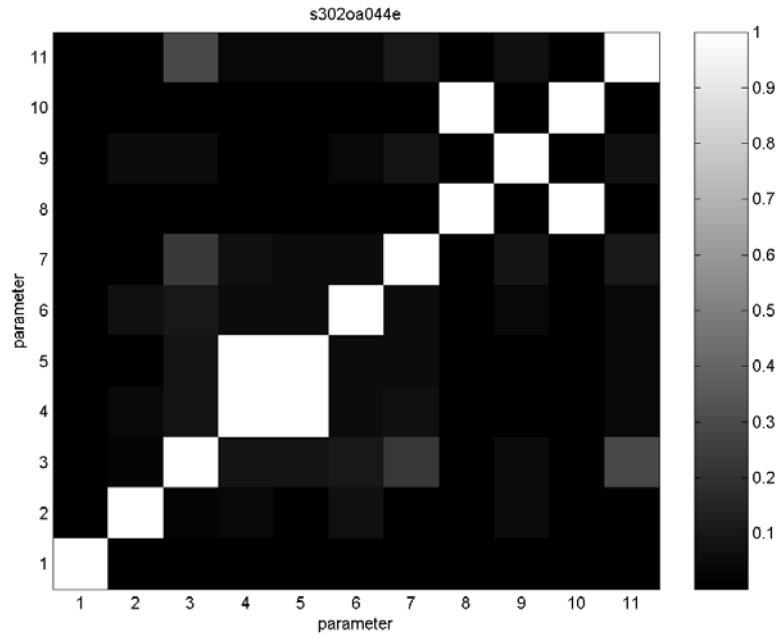


Figure 4.6 Magnitude of correlation coefficients of the eleven parameters included in the inversion at site S02. A weak colour (white) indicates strong correlation.

4.4.3 Alternative models

A few alternative parameterisations of the seabed and sets of inversion parameters were tried for subsequent inversions of the same set of data. For one series of inversions, the water depth and parameters of the halfspace were either fixed to baseline values or included in the inversions. Results are summarised in Table 4.7. The match was slightly improved when parameters of the halfspace were also included in the inversion, thus increasing the number of inversion parameters to fourteen.

Water Depth	Halfspace	Inversion Parameters	Model	Match [dB]
Inversion	Inversion	14		1.387
Inversion	Baseline	11	Table 4.5	1.464
Baseline	Inversion	10		1.555
Baseline	Baseline	-	Table 4.3	2.314

Table 4.7 Match at site S02 including water depth and parameters of the halfspace in the inversion.

Next a series of seabed models of reduced complexity were tried. Use of reduced-complexity models may be of interest for applications where fast and crude propagation modelling results are desired (20), at the risk of tailoring models for specific applications. Here inversions were set up using one and two-layer elastic models and an all-fluid seabed model. Average match is tabulated in Table 4.8. Match at individual frequency bands from 16 Hz - 160 Hz is plotted in Figure 4.7. The estimated model parameters are further tabulated in the Appendix.

Seabed Model	Inversion Parameters	Model	Match [dB]
Three-Layer Elastic	11	Table 4.5	1.464
Two-Layer Elastic	10	Table C.2	1.498
Elastic Halfspace	6	Table C.1	1.561
Three-Layer Fluid	10	Table C.5	1.576
Fluid Halfspace	4	Table C.3	1.559

Table 4.8 Match for inversions at site S02 using one, two and three elastic seabed layer models and an all-fluid seabed models.

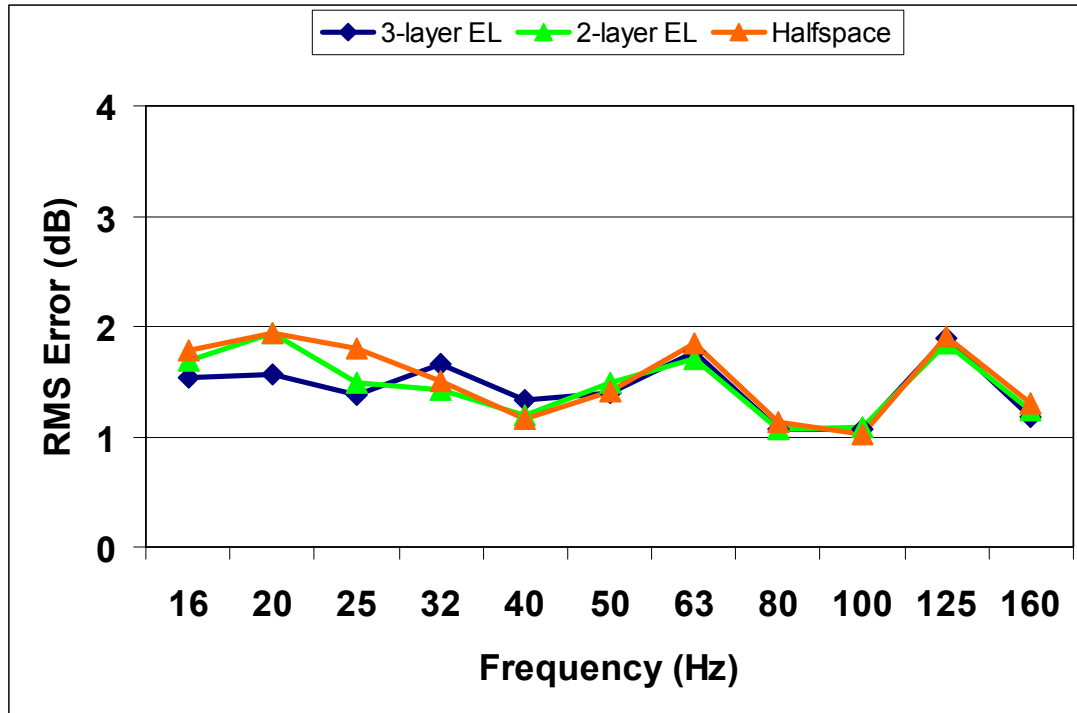


Figure 4.7 Root-mean-square transmission loss modelling error (dB) using geoaoustic model obtained from inversion using a elastic halfspace seabed model (orange line), a 2-layer elastic seabed model (green line) and a 3-layer elastic seabed model (blue line) at site S02. Data to range 20 km, 1/3-octave frequency bands from 20 Hz to 160 Hz.

The parameter estimates of the first seabed layer were in all cases quite similar to those obtained using a three-layer seabed description, with p-wave velocity of 1620 m/s and a low (< 100 m/s) s-wave velocity (no shear velocity for the all-fluid cases). These results indicate that data from this site can be modelled to good accuracy using reduced-complexity seabed models. This result may be of practical utility.

4.4.4 Few frequencies

Finally, inversions were run using data from fewer frequencies: three and five frequencies over the band 16-160 Hz, the three lowest and the three highest frequencies. A three-layer elastic seabed model was used. Results are summarised in Table 4.9 and Figure 4.8.

Frequencies [Hz]	Number of Frequencies	Match [dB]
16-160	11	1.498
16, 25,50,100,160	5	1.582
16,50,160	3	1.647
16,20,25	3	1.642
100,125,160	3	2.052

Table 4.9 Match for inversions at site S02 using data at selected frequencies. Match is averaged over all frequency bands 16-160 Hz.

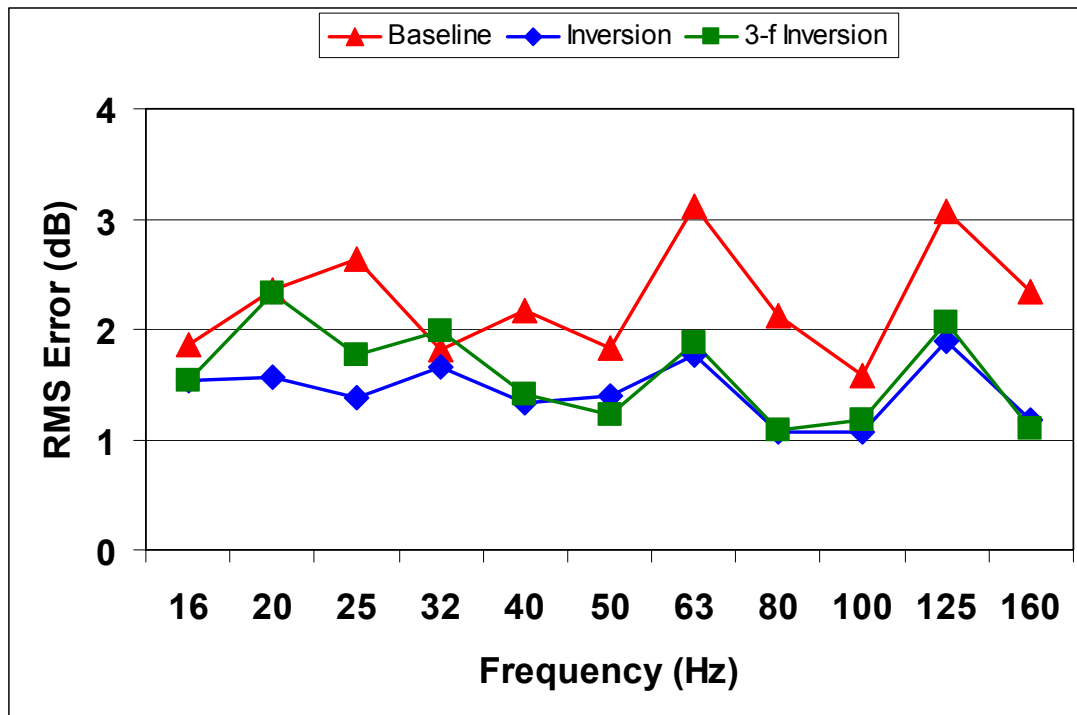


Figure 4.8 Root-mean-square transmission loss modelling error (dB) using baseline seabed model (red line) and geoacoustic model obtained from inversion using data at eleven 1/3-octave frequency bands 16 Hz-160 Hz (blue line) and three frequency bands (green line) at site S02. Data to range 20 km.

An overall good match is obtained using the five- and three-frequency models, when data at either end of the desired band is included. For these cases, the frequency bands not used in the inversion serve as control data. Also the model obtained using data from the three lowest frequencies was also quite good for this example.

4.5 Site S05

4.5.1 Baseline model

Acoustic data was collected to 20 km over a flat, slightly range-dependent layered bottom. Subcrop beneath a thin (2-20 m) layer of Quaternary sediment is a hard bedrock layer of thickness 10-30 m. Beneath the rock layer there is lower velocity rock, followed by Basement. A range-independent baseline model of Table 4.10 is assumed. The site is considered to be an “anomalous” Continental Shelf site.

Layer Type	Thickness [m]	P-wave velocity [m/s]	S-wave velocity [m/s]	P-wave attenuation [dB/λ]	S-wave attenuation [dB/λ]	Density [g/cm ³]
Water	340	1470	-	-	-	1.00
Quaternary	2	1800	300	0.80	0.80	1.80
Bedrock 1	18	6000	3200	0.30	0.15	2.60
Bedrock 2		3000	1500	0.30	0.15	2.30

Table 4.10 Baseline geoacoustic model for site S05.

Eleven parameters were included in the inversion. This also included parameters of the halfspace. Water depth and sound speed in water were fixed. Parameter interrelations were used for the following: s-wave attenuation set equal to p-wave attenuation in first sediment layer, s-wave speed set to 0.50 of p-wave speed in second layer. The inversion parameters and their search bounds are listed in Table 4.11. The total size of the search space is 10^{19} . Data from ten frequency bands (20 Hz-160 Hz) and 18 ranges (2.5-19 km), a total of 180 data points, was used in the inversions.

Parameter	Unit	Baseline Value	Search Interval	Steps
Sediment 1 thickness	m	2.0	0-20.0	64
Sediment 1 p-velocity	m/s	1800	1520-2160	128
Sediment 1 s-velocity	m/s	300	0-630	64
Sediment 1 attenuation	dB/λ	0.80	0.40-1.20	32
Sediment 1 density	g/cm ³	1.80	1.64-1.94	16
Sediment 2 thickness	m	20	2.0-28.0	64
Sediment 2 velocity	m/s	6000	4000-6200	128
Sediment 2 density	g/cm ³	2.20	1.98-2.42	16
Halfspace p-velocity	m/s	3000	2100-3900	128
Halfspace s-velocity	m/s	1500	1050-1950	128
Halfspace density	g/cm ³	2.30	2.07-2.53	16

Table 4.11 Inversion parameters for the site S05 model, baseline model values, search intervals and number of discretization steps.

4.5.2 Inversion results

Layer	Thickness [m]	P-wave velocity [m/s]	S-wave velocity [m/s]	P-wave attenuation [dB/λ]	S-wave attenuation [dB/λ]	Density [g/cm ³]
water	340	1470		-	-	1.00
Sediment 1	2.5	<i>1862</i>	<i>50</i>	<i>0.55</i>	<i>0.55(e)</i>	<i>1.92</i>
Sediment 2	8.6	<i>5177</i>	<i>2588(e)</i>	0.10	0.10	<i>2.34</i>
Halfspace		<i>2142</i>	<i>1375</i>	0.10	0.10	<i>2.53</i>

Table 4.12 Geoacoustic model from inversion of transmission loss data at site S05. Parameters in italics were included in the inversion; other parameters were fixed to nominal. A star () indicates estimate at limit of search interval, an (e) indicates a linked parameter.*

The model obtained from inversion (GA-max estimates) is shown in Table 4.12. The model seems physically reasonable; a few comments are in place:

- sediment layer: the p-wave velocity is high. From the observation that the environment is range-dependent with portions of the track possibly exposed to bedrock, a high average velocity can be expected. The s-wave velocity is low. For a thin layer as here a maximum value of 100 m/s can be expected.
- halfspace: s-wave velocity lower than sound speed in water, and a high s- to p-velocity ratio (0.64). The low s-wave velocity estimate can be explained as due to the introduction of a low-frequency loss mechanism. A high density and low p-wave velocity combined can yield correct impedance.

The match with data has improved from 5.46 dB (baseline model) to 2.16 dB (inversion model). Match at the individual frequency bands from 20 Hz to 160 Hz is plotted in Figure 4.12. The match varies between 1.5 dB and 3 dB, with an average of 2.16 dB. The improvement in match over the baseline model is most prominent at frequency bands below 100 Hz where in fact the error has been reduced from up to 12 dB to below 3 dB. Measured and modelled transmission loss is plotted in Figure 4.9. The a posteriori probability distributions for the inversion parameters are plotted in Figure 4.10. The estimated parameter values and their standard deviations are listed in Table 4.13.

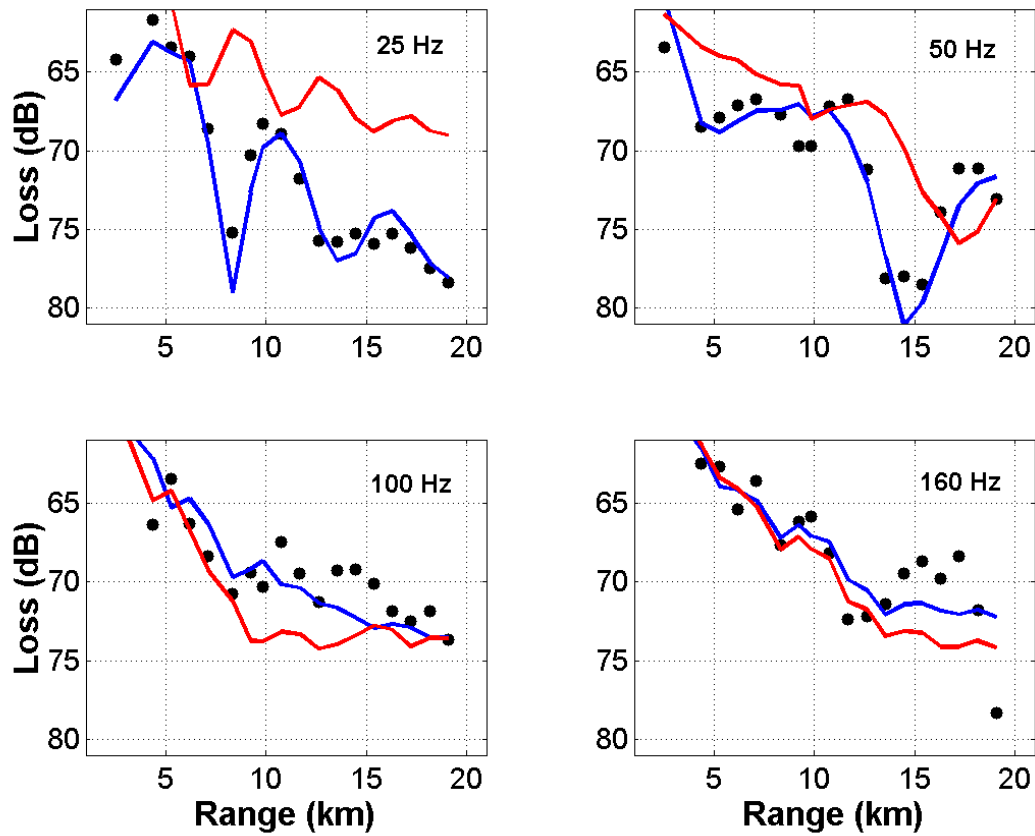


Figure 4.9 Measured and modelled transmission loss (dB) versus range (km) at site S05. Frequencies 25 Hz, 50 Hz, 100 Hz and 160 Hz. Data (black dots), modelled loss using geoacoustic model from inversion (blue line) and baseline geoacoustic model (red line).

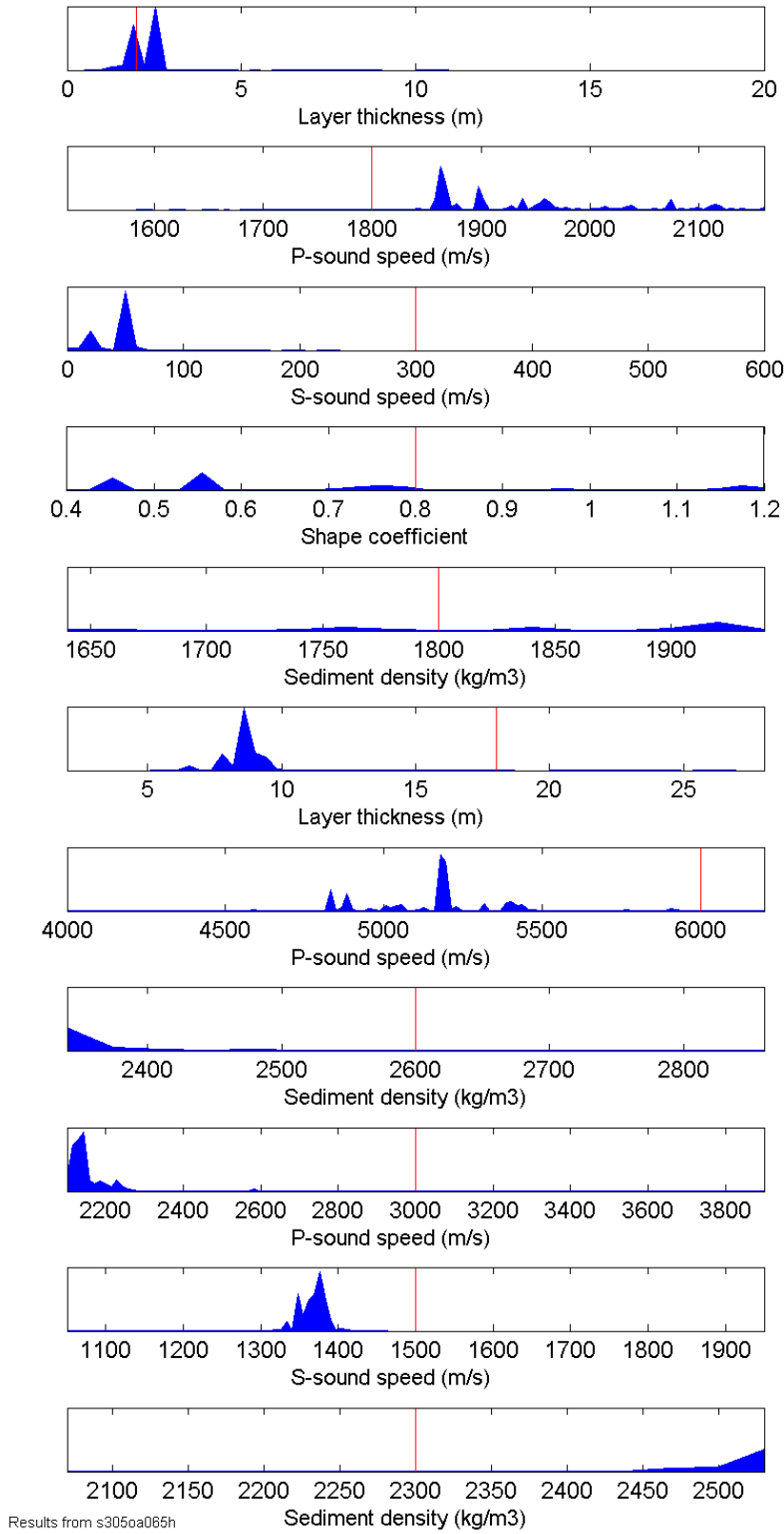


Figure 4.10 Marginal a posteriori probability densities for inversion parameters at site S05.

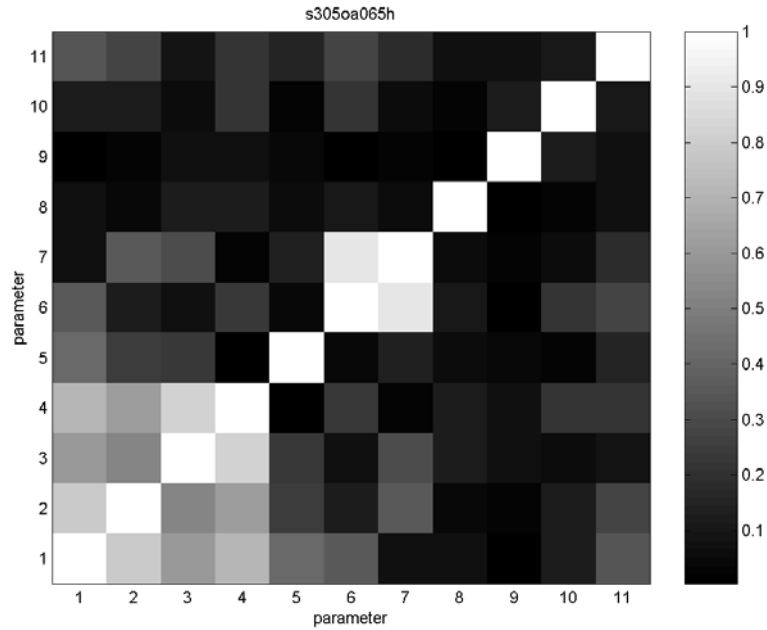


Figure 4.11 Magnitude of correlation coefficients of the eleven parameters included in the inversion at site S05. A weak colour (white) indicates strong correlation.

Parameter	Unit	Baseline Value	Inversion Estimate	Standard Deviation
Sediment 1 thickness	m	2.0	2.54	0.019
Sediment 1 p-velocity	m/s	1800	1862	0.141
Sediment 1 s-velocity	m/s	300	50	0.032
Sediment 1 attenuation	dB/ λ	0.80	0.55	0.310
Sediment 1 density	g/cm ³	1.80	1.92	0.326
Sediment 2 thickness	m	20	8.6	0.027
Sediment 2 velocity	m/s	6000	5177	0.109
Sediment 2 density	g/cm ³	2.20	2.34	0.077
Halfspace p-velocity	m/s	3000	2142	0.044
Halfspace s-velocity	m/s	1500	1375	0.018
Halfspace density	g/cm ³	2.30	2.53	0.058

Table 4.13 Model parameters at S05: baseline values, estimated by inversion of transmission loss data, and standard normalised deviation of estimates.

The four best estimated parameters, in terms of a low standard deviation, are the thickness of the first and second sediment layers and the s-wave velocities of the third and first sediment layers. The magnitudes of the correlation coefficients between the inversion parameters are plotted in Figure 4.11. The most strongly correlated parameters are: all four parameters of the first seabed layer and the thickness and p-wave velocity of the second seabed layer. It is thus indicated that the individual parameters of the first seabed layer are not well resolved, yet their combined effect on the transmission loss as measured at this site may be well modelled.

4.5.3 Alternative models

Inversions were rerun with two and one layer elastic seabed models, with wider search bounds on the geoacoustic parameters. Water depth was set to the baseline value for all these inversions. An inversion was also run with the halfspace fixed to baseline values. All-fluid models can not be used at this site. Results are shown in Table 4.14 and Figure 4.12.

Seabed Model	Inversion Parameters	Model	Match [dB]
Three-Layer Elastic	10	Table 4.12	2.130
Three-Layer Elastic Baseline Halfspace	8	Table C.8	3.238
Two-Layer Elastic	7	Table C.7	3.139
Elastic Halfspace	4	Table C.6	3.085
Baseline	-	Table 4.10	5.460

Table 4.14 Match for inversions at site S05 using alternative seabed models (all elastic layers).

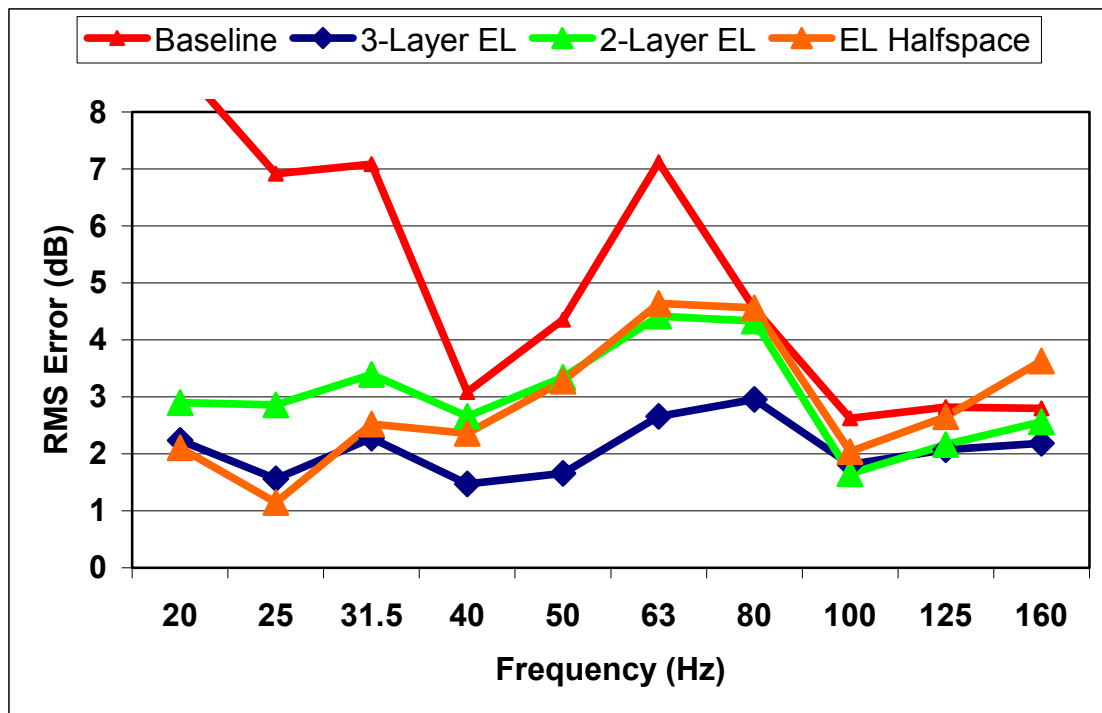


Figure 4.12 Root-mean-square transmission loss modelling error (dB) using baseline seabed model (red line) geoacoustic model obtained from inversion using a elastic halfspace seabed model (orange line), a 2-layer elastic seabed model (green line) and a 3-layer elastic seabed model (blue line) at site S05. Data to range 20 km, 1/3-octave frequency bands from 20 Hz to 160 Hz.

The parameter estimates obtained in these cases are listed in Appendix C. It is noted that the overall best match is obtained using a three-layer elastic seabed model when also inverting for parameters of the halfspace. This is also the model that corresponds to geophysical information on the seabed layering at this site. Results will not be further discussed here.

4.5.4 Inversion in segments

The inversion was rerun using data in three segments in range: 0-8 km, 8-12 km and 12-20 km. A three-layer range-independent seabed model description was used for each run, with parameters of all layers included in the inversions. Estimates of parameters of the first sediment layer are shown in Table 4.15.

Segment	Ranges [km]	Number of sources	Estimate Sediment Thickness	Estimate Sediment p-/s-vel	Match [dB]
First	2-8	6	8.6	p1615 s240	1.706
Second	8-12	6	2.2	p1978 s50	1.452
Third	12-20	7	2.5	p2018 s0	2.384
All	2-20	19	2.5	p1862 s50	2.138

Table 4.15 Match for inversions at site S05 using data from three segments in range and for all data combined. A three-layer elastic seabed range-independent model was used. Ranges in second column indicate those from which data was taken. Model parameters obtained by inversion for the first sediment layer only are provided. Match is for inversion model, for data included in the inversions only.

It is observed that a considerably different model for the first seabed layer is obtained when using data of the first segment alone. The seismic section of this segment indicates a thicker deposit of Quaternary sediment (4-20 m), which is in agreement with the results from the inversion. Sediment thickness at the second segment is thin (from an estimated <1 m to 4 m), also in accordance with the model obtained from inversion of data from this segment. Data from the third segment are affected also by the properties of the second segment, thus although a thicker sediment layer (4-20 m) is indicated in the seismic section, a thin-layer model corresponding to the one found in inversion of segment two data is obtained in the inversion. Inversion of data in a range-dependent environment should eventually be done using a range-dependent environment model and by use of a full-fledged range-dependent forward model, in this case a model that accounts for shear-dependent loss and/or propagates shear waves correctly.

4.6 Summary

Two transmission loss data sets from the Continental Shelf, each of about two hundred data points (ten frequencies and twenty ranges) were used for geoacoustic inversion. Improved-match seabed models in reasonable agreement with data from other geophysical methods were obtained. A reduced-complexity seabed model can be used at the first site.

5 SUMMARY

This study consisted of two parts. In the first part, synthetic acoustic data for a set of typical Continental Shelf seabed environments was inverted for geoacoustic parameters. A standard set of test cases was used and augmented with two cases incorporating effects of thin geoacoustic layers. It was found that transmission loss data could indeed be used for the purpose, with the possibility to recover key geoacoustic parameters or combinations of such. As expected, use of TL data for inversion is inferior to the use of complex pressure field data with the Bartlett processor, though for thin-layer environments TL data was indicated to yield results of comparable quality. The genetic algorithm global search method of SAGA was used. This tool performed well also in the difficult parameter spaces encountered where thin-layer effects are present.

The second part applied the inversion method to two transmission loss data sets acquired at the Continental Shelf. Data recorded at a single hydrophone in the water column from twenty sources in range (2-20 km) and ten one-third octave frequency bands (20-160 Hz), thus a total of about two hundred data points was used. Baseline geoacoustic models constructed from available and interpreted geophysical data were set up at each site. These models were also used to assess parameter sensitivities prior to inversion. The importance of baseline models, in particular of the layering of the seabed, is stressed. Reasonable good-match seabed models were obtained by inversion of TL data both for a soft sediment site and for an anomalous thin-layer site, with parameter estimates not in strong disagreement with values obtained by other geophysical methods. Lack of further “ground truth” data, whether obtained by geophysical methods or by matched-field inversion of other types of acoustic data, prevents further assessment of the parameter estimates obtained. It could be argued that little has been gained over the mere use of a baseline model at the first site, with an overall reduction of 1.0 dB in modelling error, but it should be remembered that these results were obtained using little a priori information except for the layering of the seabed and with wide search bounds on the geoacoustic parameters. At this site, reduced-complexity seabed models were seen to yield comparable match with data. At the anomalous site a significant improvement in match was obtained, with an overall reduction of 3.0 dB in modelling error and up to 12 dB for individual data points. The geoacoustic model obtained from inversion at this site is difficult to interpret, as there are several seabed loss mechanisms in effect, and the contribution of each of these is difficult to isolate.

The results presented in this report support the development of an improved acoustic modelling and prediction capability for the Continental Shelf. The use of transmission loss data has recently attracted interest for rapid assessment of passive sonar conditions in unknown or less known areas. Refinements and extensions of the inversion method applied in this report should be of interest also in this respect.

References

- (1) W A Kuperman and F B Jensen (eds.) (1980): Bottom-interacting ocean acoustics, NATO Conference Series, Plenum Press.
- (2) N R Chapman and M Taroudakis (eds.) (2000): Geoacoustic inversion in shallow water, *J Comp Acoust.* Vol. 8, No. 2
- (3) N R Chapman and A Tolstoy (eds.) (1998): Benchmarking geoacoustic inversion methods, *J Comp Acoust.* Vol. 6, No. 1&2
- (4) G J Heard, D Hannay and S Carr (1998): Genetic algorithm inversion of the 1997 geoacoustic inversion workshop test case data, *J Comp Acoust.* Vol. 6, 61-71.
- (5) L Abrahamsson and B L Andersson (2000): Identification of seabed geoacoustic parameters from transmission loss data, FOA R--00-01752-409--SE
- (6) J Pihl, P Söderberg, A Wester, V Westerlin (1999): A method for on-site determination of geo-acoustic parameters, FOA-R--99-01281-409--SE
- (7) P Gerstoft (2001): SAGA User Manual 4.1: An inversion software package, SACLANT Undersea Research Centre, La Spezia, Italy and Marine Physical Laboratory, Scripps Institution of Oceanography, University of California at San Diego, USA
- (8) H Schmidt (2000), OASES v2.0 User Manual, Massachusetts Institute of Technology.
- (9) C H Harrison and J A Harrison (1995): A simple relationship between frequency and range averages for broadband sonar, *J Acoust Soc Am* **97**, 2, 1314-7.
- (10) F B Jensen et al. (1994): Computational Ocean Acoustics, Springer-Verlag.
- (11) D M F Chapman (2001): What are we inverting for? in M I Taroudakis and G N Makrakis (eds.), Inverse problems in underwater acoustics, Springer Verlag, p.1-14.
- (12) D Tollefsen (1998): Thin-sediment shear-induced effects on low-frequency broadband acoustic propagation in a shallow continental sea, *J. Acoust. Soc. Am.* **104**, 5, 2718-26.
- (13) J M Hovem, C E Solberg and D Tollefsen (2001): Acoustic propagation anomalies caused by thin geoacoustic layers, OCEANS 2001, MTS-0-933957-9
- (14) P Ratilal, P Gerstoft and J O Goh (1998): Subspace approach to inversion by genetic algorithms involving multiple frequencies, *J Comp Acoust.* Vol. 6, 99-115.
- (15) M R Fallat and S E Dosso (1998): Geoacoustic Inversion for the Workshop '97 Benchmark Test Cases Using Simulated Annealing, *J Comp Acoust.* Vol. 6, 29-44.
- (16) D P Knobles et al. (1998): The Inversion of Ocean Waveguide Parameters Using a Nonlinear Least Squares Approach, *J Comp Acoust.* Vol. 6, 83-98.

- (17) S E Dosso, M J Wilmut and A-L S Lapinski (2001): An Adaptive-Hybrid Algorithm for Geoacoustic Inversion, *IEEE Journal of Oceanic Engineering*. Vol. 26, 324-36.
- (18) M D Max, R Hollett, J Fawcett and J Berkson (1996): Transmission-Loss characteristics and geoacoustic model for an outer Albanian Continental Shelf platform in the south-east Adriatic Sea, SACLANT Undersea Research Centre, La Spezia, Memorandum SM-300
- (19) C L Siedenburg et al (1995): Iterative full-field inversion using simulated annealing in O Diachok et al. (eds.), *Full Field Inversion Methods in Ocean and Seismo-Acoustics*, Kluwer Academic, p.121-126
- (20) P A Baxley (2002): Matched-Field processor optimisation using simple bottom models, *The First International Conference on Inverse Problems: Modeling and Simulation*, Fethiye, Turkey, p. 26

A TWO-PAGE ABSTRACT⁶

Propagation of low-frequency sound in shallow water is in general strongly dependent on the geoacoustic properties of the seabed, and rapid and inexpensive methods for estimating these parameters are desired. Recent developments of matched-field inversion (MFI) techniques in underwater acoustics have brought several advanced methods for this purpose [1]. While most applications of MFI treat pressure fields directly, the present work makes use of frequency-band averaged transmission loss (TL) data [2]. Data of this type is readily available from sound propagation measurements on the Continental Shelf.

Methods

Acoustic and geophysical data.

Experiments took place at water depths of about 350 m on the Continental Shelf. Explosives (SUS) charges were detonated at ranges of 2 km to 20 km (interval 1 km) from a deployed hydrophone receiver in the water column. Acoustic data was processed for TL in 1/3-octave frequency bands from 20 Hz to 160 Hz. Supporting geophysical data acquired at sea consisted of bathymetry and seismic profiles along the experiment tracks, a CTD profile of the sound speed in water and a wide-angle bottom refraction (WABR) measurement inverted for a compressional velocity versus depth profile in the seabed.

Seabed models.

Initial or *baseline* seabed models were set up using available and acquired a priori geophysical information. For the sites considered here, models using three homogeneous elastic seabed layers were used. Layer thickness and compressional (p-) wave velocities were based on data described above. In addition, a priori less determined but potentially influential parameters such as the shear (s-) speeds, densities and p- and s-wave attenuations of each layer were included in the set of model parameters. Including also the mean water depth along the experiment track, the total number of model parameters for a three-layer elastic seabed is eighteen.

Forward model, fitness function and search algorithm.

Modelled (simulated) acoustic data was produced using the range-independent version of the OASES forward propagation model [3] for layered fluid-solid media. The source and receiver depths, source ranges and sound speed profile in water was fixed to nominal values. Seabed model parameters were varied between individual runs of the forward model as described below.

Modelled TL data was matched with measured data using a modified least-squares "fitness" function

$$E(\mathbf{m}) = \sqrt{\frac{1}{N} \sum_{j,f} [\text{TL}_{j,f}^{\text{OBS}} - \text{TL}_{j,f}(\mathbf{m})]^2} \quad (1)$$

where the summation extends over N data points, $\text{TL}_{j,f}^{\text{OBS}}$ the measured and $\text{TL}_{j,f}(\mathbf{m})$ the simulated transmission loss (both in dB) for range index j and frequency index f , the latter for a seabed model \mathbf{m} .

A global search was set up over candidate seabed models \mathbf{m} . The number of search parameters was reduced from eighteen to eight by fixing less influential parameters, as assessed by one-dimensional sensitivity studies prior to the inversions. With sixty-four test values per parameter (over relatively wide search intervals), the total size of the parameter space is 10^{14} , which precludes use of an exhaustive search. The search for a (set of) best-fit model(s) is facilitated using the global search genetic algorithm of the SAGA inversion tool [4]. Inversions were set up for a preset number model runs, for this work 16.000 runs divided among eight independent populations was used. Further parameters of the genetic algorithm were set to recommended standards [4]. The execution time of a typical inversion run was six hours on a HP700-series twin-processor computer.

Results

Results are shown for two test sites, the first modelled as two thick (80-120 m) layers of relatively soft sediment over a hard consolidated sediment halfspace, the second as two thin (2-20 m) layers (soft sediment over hard bedrock) on top of a consolidated sediment halfspace. Both environments were treated as range independent. The second environment is considered "anomalous". Characteristics of the acoustic propagation and results from forward modelling of data at the second site have been discussed in [5].

⁶ Proceedings of the 25th Scandinavian Symposium on Physical Acoustics at Ustaoset, January 27-30, 2002.

In Figure 1 results from modelling at the two sites is shown. The panels show measured and modelled transmission loss versus range using the baseline seabed model and the seabed model obtained from inversion, for four frequency bands from 20 Hz to 160 Hz. Equation (1) was also used as a final measure of total "fitness" between measured and modelled data. At site 1, total fitness improved from 2.3 dB (baseline model) to 1.5 dB (inversion model). At site 2, fitness improved from 5.5 dB to 2.1 dB.

Results from the first site (left panel) show that even the baseline model captures most of the "structure" seen in the TL data, at only slightly offset values. The most significant change in the seabed model obtained from inversion was a reduction of the p-wave velocity of the first seabed layer by 10%. It may be argued that little has been gained by inverse modelling at this site, but it should be remembered that the inversion model has been obtained using a modest amount of a priori information and wide search bounds on the seabed model parameters.

Results from the second site show a substantial improvement in fitness at frequency bands below 80 Hz (e.g. an average of in excess of 6 dB at 25 Hz) using the seabed model obtained from inversion. In this case, structure as seen in data is not modelled well by the baseline model. This structure arises from three prominent shear-dependent seabed loss mechanisms; two effects are related to properties of the first two layers [5], the third arises from transmission through these layers and subsequent loss due to conversion to s-waves in the halfspace.

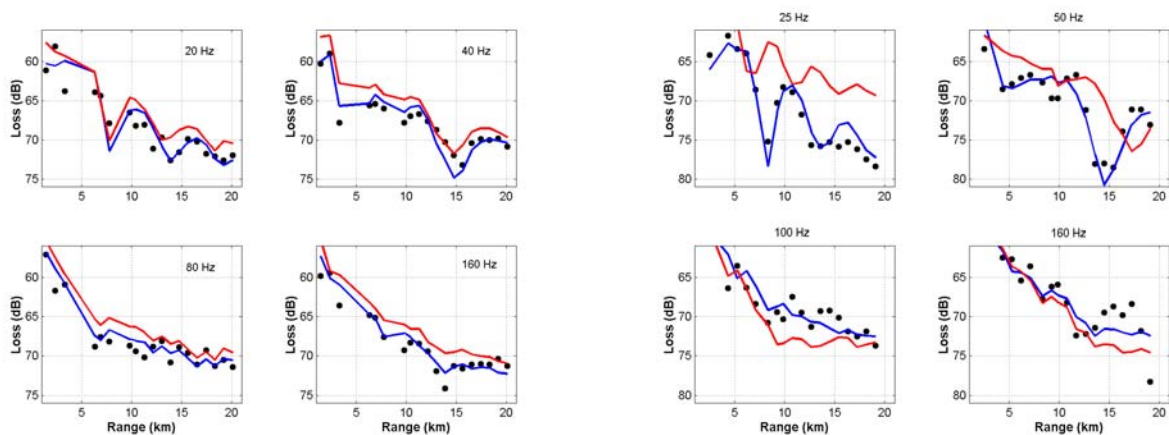


Figure 1. Measured and modelled transmission loss at two shallow water sites on the Continental Shelf. "Thick sediment" site (left panel) and "anomalous" site (right panel). Data (black dots) at four 1/3-octave frequency bands between 20 and 160 Hz. Modelled loss using input from an initial seabed model based on a priori geophysical information (red line) and seabed model obtained by inversion of acoustic TL data (blue line).

Discussion and summary

The seabed models used in this study consisted of three elastic layers, with a total of eight model parameters included in the inversion (not the same set) at each site. The best-fit estimated geoacoustic model parameters obtained by inversion will not be quoted here, but were in general not in strong disagreement with data obtained by other geophysical methods at the sites. Further work not shown has included the use of seabed models of reduced complexity (fewer layers) and inversion using subsets of the data (fewer frequencies). Future work is intended to address aspects of range-dependence in the modelling and inversion scheme.

In summary, it has been shown that transmission loss data collected for the characterisation of low-frequency (20-160 Hz) long-range propagation in shallow water can be used in an inverse modelling procedure to obtain estimates, albeit crude, of seabed geoacoustic parameters relevant to this propagation. The genetic algorithm global search method of SAGA has provided a useful tool in this procedure. The method is relatively rapid and inexpensive.

References

- [1] R Chapman and M Taroudakis (eds.), "Geoacoustic inversion in shallow water," J Comp Acoust, vol 8 No 2, June 2000.
- [2] L Abrahamsson and B L Andersson, "Identification of seabed geoacoustic parameters from transmission loss data," FOA Methodology Report FOA-R--0-01752-409--SE, Stockholm, December 2000.
- [3] H Schmidt, "SAFARI: Seismo-Acoustic Fast field Algorithm for Range-Independent environments," Report SR-113, SACLANT Undersea Research Centre, La Spezia, Italy, 1988.
- [4] P Gerstoft, "SAGA User Manual 3.0: An inversion software package", SACLANT Undersea Research Centre, La Spezia, Italy and Marine Physical Laboratory, University of California at San Diego, January 1999. [See also <http://oalib.saic.com>]
- [5] J M Hovem, C E Solberg and D Tollefsen, "Acoustic propagation anomalies caused by thin geoacoustic layers," Oceans 2001, MTS-0-933957-9

B TEST CASES

Additional results for the synthetic test cases are presented. The source-sensor configurations are listed in Table B.1. EL test cases and model parameter estimates are listed in section B.1. CS test cases and model parameter estimates are listed in section B.2.

	Label	Sensors or sources				Frequencies [Hz]	Processor
		Range [km]	Depth [m]	Quantity	Spacing [m]		
	VLA	1.0	5-100	20	5.0	32,63,160	Bartlett
	HLA-1	1.0-3.0	100	20	50-200	32,63,160	Bartlett
	HLA	3.0-5.0	100	20	50-200	32,63,160	Bartlett
	TL-O2	0.5-5.0	20	16	300	32,63	TL 1/3-octave
	TL-O3	0.5-5.0	20	16	300	32,63,160	TL 1/3-octave
	TL-O8	0.5-5.0	20	16	300	32-160	TL 1/3-octave
	TL-O10	0.5-5.0	20	16	300	25-200	TL 1/3-octave
	TL-nb	0.5-5.0	75	91	50	32,63,160	TL multi-tone
	TL-nb-c	0.5-5.0	75	91	50	25,50,100	TL multi-tone
	TL-nb-d	0.5-5.0	75	91	50	32,63,125,250	TL multi-tone

Table B.5.1 Source-sensor configurations, processors and processing frequencies.

B.1 EL cases

Parameter	Search interval	EL-A	EL-B	EL-C
Sediment thickness [m]	30.0-80.0	55.1365	75.5999	34.8417
Sediment p-wave speed [m/s]	1650-1750	1669.35	1697.81	1674.78
Sediment s-wave speed [m/s]	100-300	130.630	134.347	180.148
Sediment density [g/ccm]	1.80-2.10	1.85324	1.88254	1.83790
Halfspace p-wave velocity [m/s]	1700-1900	1728.47	1839.85	1747.80
Halfspace s-wave velocity [m/s]	200-500	406.911	214.316	438.752
Halfspace density [g/ccm]	2.00-2.20	2.06771	2.14580	2.05498

Table B.5.2 Inversion parameters, search intervals and nominal values for EL test cases.

Scenario	h_{sed} (m)	c_{sed} (m/s)	$c_{sh,sed}$ (m/s)	ρ_{sed} (g/ccm)	c_{hsp} (m/s)	$c_{sh,hsp}$ (m/s)	ρ_{hsp} (g/ccm)	MADE
TRUE-A	55.14	1669.35	130.63	1.853	1728.47	406.91	2.068	0.000
VLA	54.50	1668.00	180.00	1.881	1728.00	431.00	2.100	0.087
HLA	55.00	1669.00	108.00	1.836	1728.00	389.00	2.002	0.081
HLA-1	55.50	1670.00	222.00	1.959	1728.00	392.00	2.050	0.138
TL-O2	54.00	1670.00	126.00	1.845	1726.00	314.00	2.002	0.104
TL-O3	56.00	1669.00	162.00	1.851	1730.00	461.00	2.024	0.085
TL-O8	55.00	1669.00	148.00	1.851	1730.00	452.00	2.122	0.076
TL-O10	54.00	1671.00	152.00	1.803	1720.00	206.00	2.188	0.232
TL-nb	54.50	1669.00	160.00	1.839	1728.00	377.00	2.066	0.046
TL-nb-d	55.50	1670.00	166.00	1.890	1728.00	371.00	2.030	0.089

Table B.5.3 True parameter values and estimates, case EL-A, scenarios listed in Table B.1

Scenario	h_{sed} (m)	c_{sed} (m/s)	$c_{sh,sed}$ (m/s)	ρ_{sed} (g/ccm)	c_{hsp} (m/s)	$c_{sh,hsp}$ (m/s)	ρ_{hsp} (g/ccm)	MADE
TRUE-B	75.60	1697.81	134.35	1.883	1839.85	214.32	2.146	0.000
VLA	77.00	1701.00	162.00	2.064	1826.00	254.00	2.198	0.181
HLA	72.50	1694.00	118.00	1.830	1822.00	485.00	2.182	0.218
HLA-1	75.50	1697.00	112.00	1.851	1851.00	389.00	2.162	0.135
TL-O2	76.50	1698.00	290.00	2.085	1840.00	203.00	2.048	0.286
TL-O3	76.50	1698.00	300.00	2.067	1842.00	200.00	2.028	0.302
TL-O8	73.50	1692.00	290.00	2.088	1826.00	485.00	2.058	0.425
TL-O10	71.50	1700.00	300.00	2.004	1736.00	200.00	2.190	0.304
TL-nb	77.00	1700.00	216.00	1.962	1828.00	476.00	2.162	0.248
TL-nb-c	33.50	1698.00	100.00	1.845	1708.00	203.00	2.190	0.294

Table B.5.4 True parameter values and estimates, case EL-B, scenarios listed in Table B.1

Scenario	h_{sed} (m)	c_{sed} (m/s)	$c_{sh,sed}$ (m/s)	ρ_{sed} (g/ccm)	c_{hsp} (m/s)	$c_{sh,hsp}$ (m/s)	ρ_{hsp} (g/ccm)	MADE
TRUE-C	34.84	1674.78	180.15	1.838	1747.80	438.75	2.055	0.000
VLA	35.50	1681.00	186.00	1.842	1724.00	308.00	2.182	0.187
HLA	43.50	1676.00	114.00	1.800	1706.00	485.00	2.182	0.234
HLA-1	35.00	1681.00	158.00	1.839	1722.00	209.00	2.198	0.256
TL-O2	63.50	1650.00	300.00	1.800	1700.00	224.00	2.174	0.442
TL-O3	63.00	1650.00	300.00	1.800	1700.00	236.00	2.176	0.437
TL-O8	78.50	1650.00	300.00	1.800	1700.00	485.00	2.002	0.358
TL-O10	80.00	1669.00	300.00	1.842	1700.00	300.00	2.006	0.360
TL-nb	30.00	1674.00	290.00	1.893	1710.00	365.00	2.190	0.278
TL-nb-d	35.00	1676.00	284.00	1.968	1714.00	500.00	2.006	0.227

Table B.5.5 True parameter values and estimates, case EL-C, scenarios listed in Table B.1

B.2 CS cases

Parameter	Search interval	CS-B	CS-D
Sediment thickness [m]	0.0-10.0 B 0.0-20.0 D	2.00	10.00
Sediment p-wave speed [m/s]	1650-1750	1700.0	1700.0
Sediment s-wave speed [m/s]	0-300	200.00	200.00
Sediment density [g/ccm]	1.70-2.10	1.8000	1.8000
Halfspace p-wave velocity [m/s]	3960-4960	4700.0	4700.0
Halfspace s-wave velocity [m/s]	1800-2400	1900.0	2100.0
Halfspace density [g/ccm]	2.25-2.55	2.4000	2.4000

Table B.5.6 Inversion parameters, search intervals and nominal values for CS test cases.

Scenario	h_{sed} (m)	c_{sed} (m/s)	$c_{\text{sh,sed}}$ (m/s)	ρ_{sed} (g/ccm)	c_{hsp} (m/s)	$c_{\text{sh,hsp}}$ (m/s)	ρ_{hsp} (g/ccm)	MADE
TRUEb	2.00	1700.00	200.00	1.800	4700.00	1900.00	2.400	0.000
VLA	1.90	1684.00	192.00	1.870	4830.00	1896.00	2.360	0.092
HLA	2.10	1682.00	210.00	1.780	4850.00	1902.00	2.405	0.063
HLA-1	2.10	1700.00	207.00	1.770	4600.00	1908.00	2.460	0.060
TL-O2	2.00	1650.00	201.00	1.700	4410.00	1890.00	2.400	0.151
TL-O3	0.20	1748.00	198.00	1.950	4270.00	2274.00	2.500	0.347
TL-O8	2.00	1694.00	201.00	1.700	4960.00	1890.00	2.300	0.132
TL-nb	2.00	1736.00	198.00	1.770	4610.00	1896.00	2.420	0.086
TL-nb-c	2.00	1685.00	201.00	1.830	4700.00	1902.00	2.420	0.043

Table B.5.7 True parameter values and estimates for case CS-B for scenarios listed in Table B.1.

Scenario	h_{sed} (m)	c_{sed} (m/s)	$c_{\text{sh,sed}}$ (m/s)	ρ_{sed} (g/ccm)	c_{hsp} (m/s)	$c_{\text{sh,hsp}}$ (m/s)	ρ_{hsp} (g/ccm)	MADE
TRUEd	10.00	1700.00	200.00	1.800	4700.00	2200.00	2.400	0.000
VLA	10.20	1701.00	204.00	1.770	4490.00	2208.00	2.410	0.052
HLA	9.80	1695.00	198.00	1.900	4280.00	2232.00	2.375	0.125
HLA-1	9.00	1676.00	69.00	1.700	4280.00	2178.00	2.300	0.252
TL-O2	9.80	1715.00	195.00	1.860	4480.00	2208.00	2.435	0.097
TL-O3	10.20	1694.00	204.00	1.770	4590.00	2202.00	2.450	0.063
TL-O8	10.20	1697.00	204.00	1.730	4730.00	2196.00	2.490	0.081
TL-nb	9.60	1694.00	84.00	1.710	4010.00	2214.00	2.400	0.201
TL-nb-d	10.00	1699.00	123.00	1.770	3960.00	2226.00	2.400	0.161

Table B.5.8 True parameter values and estimates for case CS-D for scenarios listed in Table B.1.

C SEABED MODELS

Geoacoustic parameter estimates obtained by inversion of transmission loss data from sites S02 and S05 using various seabed models of reduced complexity are listed. Parameters in italics were included in the inversions; these are the GA-max estimates obtained from SAGA. A star (*) indicates an estimate at the limit of the search interval; an (e) indicates that s-wave parameters are linked to the p-wave parameters for this parameter and layer.

C.1 Site S02

Layer	Thickness [m]	P-wave velocity [m/s]	S-wave velocity [m/s]	P-wave attenuation [dB/λ]	S-wave attenuation [dB/λ]	Density [g/cm ³]
Water	343.5	1470		-	-	1.00
Halfspace		1623	0*	0.81	1.17	2.26*

Table C.1 Elastic halfspace geoacoustic model from inversion at site S02.

Layer	Thickness [m]	P-wave velocity [m/s]	S-wave velocity [m/s]	P-wave attenuation [dB/λ]	S-wave attenuation [dB/λ]	Density [g/cm ³]
Water	343.9	1470		-	-	1.00
Sediment	46.6	1610	80	0.65	0.99	2.22
Halfspace		2048	1696	0.10	0.10	2.39

Table C.2 Two-layer elastic geoacoustic model from inversion at site S02.

Layer	Thickness [m]	P-wave velocity [m/s]	S-wave velocity [m/s]	P-wave attenuation [dB/λ]	S-wave attenuation [dB/λ]	Density [g/cm ³]
Water	343.0*	1470		-	-	1.00
Halfspace		1614	-	0.73	-	2.26*

Table C.3 Fluid halfspace model from inversion at site S02.

Layer	Thickness [m]	P-wave velocity [m/s]	S-wave velocity [m/s]	P-wave attenuation [dB/λ]	S-wave attenuation [dB/λ]	Density [g/cm ³]
Water	344.8	1470		-	-	1.00
Sediment	65.5	1636	-	0.94	-	2.10
Halfspace	-	2079	-	0.10	-	1.98*

Table C.4 Two-layer all-fluid model from inversion at site S02.

Layer	Thickness [m]	P-wave velocity [m/s]	S-wave velocity [m/s]	P-wave attenuation [dB/ λ]	S-wave attenuation [dB/ λ]	Density [g/cm ³]
Water	345.3	1470		-	-	1.00
Sediment 1	160*	1650	-	1.02	-	2.06
Sediment 2	122	2524	-	0.10	-	2.10
Halfspace		3666	-	0.10	-	2.16

Table C.5 Three-layer all-fluid model from inversion at site S02.

C.2 Site S05

Layer	Thickness [m]	P-wave velocity [m/s]	S-wave velocity [m/s]	P-wave attenuation [dB/ λ]	S-wave attenuation [dB/ λ]	Density [g/cm ³]
Water	340	1470		-	-	1.00
Halfspace		2480	750	0.40	0.40(e)	1.64

Table C.6 Elastic halfspace geoaoustic model from inversion at site S05

Layer	Thickness [m]	P-wave velocity [m/s]	S-wave velocity [m/s]	P-wave attenuation [dB/ λ]	S-wave attenuation [dB/ λ]	Density [g/cm ³]
Water	340	1470		-	-	1.00
Sediment	13.6	1610	220	1.20	1.20(e)	1.94
Halfspace		4218	2109(e)	0.10	0.10	2.58

Table C.7 Two-layer elastic geoaoustic model from inversion at site S05

Layer	Thickness [m]	P-wave velocity [m/s]	S-wave velocity [m/s]	P-wave attenuation [dB/ λ]	S-wave attenuation [dB/ λ]	Density [g/cm ³]
Water	340	1470		-	-	1.00
Sediment 1	14.6	1595	230	0.94	0.94(e)	1.76
Sediment 2	28.7	4275	2137(e)	0.10	0.10	2.37
Halfspace		3000	1500	0.10	0.10	2.30

Table C.8 Three-layer elastic geoaoustic model from inversion at site S05. Parameters of halfspace fixed to baseline values.

DISTRIBUTION LIST

FFIBM
Dato: 5 desember 2002

RAPPORTTYPE (KRYSS AV)			RAPPORT NR.	REFERANSE	RAPPORTENS DATO	
<input checked="" type="checkbox"/>	RAPP	<input type="checkbox"/> NOTAT	<input type="checkbox"/> RR	2002/04608	FFIBM/836/116	5 desember 2002
RAPPORTENS BESKYTTELSESGRAD				ANTALL EKS UTSTEDT	ANTALL SIDER	
Unclassified				43	56	
RAPPORTENS TITTEL				FORFATTER(E)		
GEOACOUSTIC INVERSION ON THE CONTINENTAL SHELF: LAYERED ELASTIC SEABEDS				TOLLEFSEN Dag		
FORDELING GODKJENT AV FORSKNINGSSJEF				FORDELING GODKJENT AV AVDELINGSSJEF:		
Jarl K Johnsen				Jan Ivar Botnan		

EKSTERN FORDELING
INTERN FORDELING

ANTALL	EKS NR	TIL	ANTALL	EKS NR	TIL
2		FO/E	9		FFI-Bibl
1		v/ Oing J A Sunde	1		FFI -ledelse
1		FO/SST	1		FFIE
1		v/ KK K Aremo	1		FFISYS
1		SJKE/UVBF	1		FFIBM
1		v/ OK J Ramfjord	1		FFIN
1		KNMT/SMOPS	1		Avd ktr FFIBM/Horten
1		v/ OK S-O Hole	1		Forfattereksemplar(er)
1		FLO/SJØ	3		Restopplag til Biblioteket
1		v/ Senioring. S Mjølshes			Elektronisk fordeling:
1		FMGT			FFI-veven
1		v/ Kapt ltn J Stensaker			Jarl K Johnsen (JKJ)
1		FKS/FOHK			Torgeir Svolsbru (TSU)
1		v/ OK F Tveiten			Connie E Solberg (CES)
1		NAVOCEANO code N53			Ellen J Eidem (EJE)
1		NAVOCEANO code 531			Trond Jenserud (TJE)
		Stennis Space Centre			Knut A Søstrand (KAS)
		MS 39522-5001,USA			
1		Professor N R Chapman			
		School of Earth and Ocean Sciences			
		University of Victoria			
		Victoria BC V8W 3P6, Canada			
1		Professor I Karasalo			
		Swedish Defence Research Agency			
		Systems Technology			
		SE-172 90 Stockholm, Sverige			
1		Dr. Peter Gerstoft			
		Marine Physical Laboratory			
		Scripps Institution of Oceanography			
		University of California			
		San Diego, CA 92093-0701, USA			
1		Professor Jens M Hovem			
		NTNU			
		7491 Trondheim			

FFI-K1

Retningslinjer for fordeling og forsendelse er gitt i Oraklet, Bind I, Bestemmelser om publikasjoner for Forsvarets forskningsinstitutt, pkt 2 og 5. Benytt ny side om nødvendig.

EKSTERN FORDELING**INTERN FORDELING**

ANTALL	EKS NR	TIL	ANTALL	EKS NR	TIL
1		NERSC Edv Griegs vei 3A 5059 Bergen			
1		NGU v/Terje Thorsnes Leiv Erikssons vei 39 7491 Trondheim			
1		Professor Halvor Hobæk Universitetet i Bergen Fysisk Institutt Allégt 55 5007 Bergen			